**European Master
ERASMUS MUNDUS MASTER IN
MEMBRANE ENGINEERING**

Universidad Zaragoza

Université **Paul Sabatier** TOULOUSE III

Development of Gas/Liquid Catalytic membrane reactor

By: Endalkachew Mengistie

**A Thesis Submitted to Universidad Zaragoza
in partial fulfillment of the requirements for the degree of
Erasmus Mundus Master in Membrane Engineering (EM3E)**

Supervisor: Dr. Jean-François LAHITTE

Jun 23- 2014

Abstract

Incorporating metal nanoparticles into membranes can endow the membranes with additional specific functions. This work explores the application and synthesis of palladium nanoparticles produced based on the approaches of 'Intermatrix synthesis' inside surface functionalized polyethersulfone (PES) polymer membrane. Both commercial hollow fiber and lab made flat sheet PES membranes have been successfully modified via UV induced graft polymerization of acrylic acid monomer. Palladium nanoparticles have been synthesized by chemical reduction of palladium precursor loaded on surface modified membranes. approaches to the design of membranes modified with nanomaterials. The catalytic performance of the nanoparticles have been tested by the liquid phase reduction of p-nitrophenol using $NaBH_4$ as a reductant in flow through membrane reactor. The nanocomposite membranes containing palladium nanoparticles were catalytically efficient to achieve a nearly 100 % conversion at lower convective flow. The conversion was found to be dependent on the flux, amount of catalyst and initial concentration of nitrophenol. The amount of reductant was taken in excess, hence pseudo first order kinetic assumption would be reasonable, and the kinetic rate constants were a function of catalyst surface (amount of catalyst) and initial concentration of nitrophenol. At the grafting experimental conditions of (grafting speed of 8 m/min, 25 wt% of acrylic acid monomer and at about energy of 22 J/cm^2 of membrane), a modified membrane with nearly zero water permeability was obtained. As a model for gas/liquid contacting, Palladium embedded of this nearly 'dense' membrane was tested for hydrogenation of nitrophenol.

Acknowledgments

Contents

List of Figures

List of Symbols

A_m = membrane area (m^2)

C_0 = initial concentration of reactant in membrane feed side (mM)

C = concentration in the membrane permeate, (mM)

K_{app} = apparent first order rate constant, sec^{-1}

ε = dimensionless length of the membrane

δ = length of catalytic layer

t = time, sec

J_v = membrane flux , LMH (Lh^{-1}m^{-2})

V = linear velocity of the solution in the membrane, m/sec

A = absorbance

A_0 = initial absorbance at time t =0

w= weight of catalyst

X= conversion

r = rate constant

P_e = peclet number

D= diffusion coefficient (m^2/s)

$\emptyset$ = reaction modulus

1. General Introduction

The concept of membrane reactors (MRs), combining a membrane-based separation with a catalytic chemical reaction in one unit, dates back to 1960s[2]. Since then, MRs played an important role by improving selectivity, yield and enhancing conversion for thermodynamically limited chemical reactions in many chemical processes of industrial importance. MRs are vibrant approaches for process integration by combining reaction with membrane separation in a single unit that can offer numerous advantages as compared to conventional processes. There are mainly three approaches often used in MRs to combine membranes with chemical or biochemical reaction in order to intensify a process. These are extractor, distributor and contactor MRs. Membranes, which are semipermeable structures, are important component of MRs and can be made organic or inorganic, dense or porous, inert or catalytically active[2, 3].

Catalytic membrane reactors (CMRs) are known for more than a decade; in spite of this fact, the development of catalytic membrane (CM) is still a major challenge. Catalytic membranes can be applied for wide range of applications such as in chemical, petrochemical, and water treatment. Majority of the catalytic membranes used in industries are inorganic (either ceramic or metal), for that reason, can withstand harsh reaction conditions (high temperature and pressure, concentrated and corrosive chemicals). The main drawbacks of such CMs is high cost and frangibility[3]. Because polymers are less expensive and more flexible than ceramics and metals, it is possible to use them in CMs instead of high cost metals and ceramics. However, majority of the polymers are only suitable for mild operation conditions. For this compensation, high reactive catalysts should be impregnated inside the polymer membrane matrix. In such cases, active catalysts can compromise the demand of higher temperature. Therefore, stabilisation of active catalysts by encapsulating inside polymer membranes can help to boost /enhance the drawbacks of polymer membranes.

Metal nanoparticles (MNPs) are well known for their higher catalytic activities. They have shown a great potential in different catalytic processes. Specially, MNPs of transition metals are found to be efficient and selective catalysts for several types of catalytic reactions. This is due their higher percentage of surface atoms and associated quantum effects. However, metal nanoparticles lack chemical stability and mechanical strength. They exhibit extremely high

pressure drop or head loss in fixed-bed column operation and are not found suitable for such systems[4]. Also, MNPs tend to aggregate; this phenomenon reduces their high surface area to volume ratio and subsequently reduces effectiveness. By appropriately dispersing metal nanoparticles into surface functionalized polymer membranes, many of these shortcomings can be overcome without compromising the parent properties of the nanoparticles. Immobilization of MNPs on solid support, besides to provide a mechanical strength, it offers an option to maintain their catalytic activities by preventing unnecessary growth and aggregation. Moreover, catalytic application of MNPs is the best alternative to efficiently utilized expensive metals. Immobilization of MNPs on polymer membrane support is therefore, best strategy to overcome the drawbacks of both polymers and MNPs [5]. Theses methodology also gives rise to process intensification by combining catalysis and membrane process at the same unit.

One mechanism to stabilize MNPs inside polymer membrane matrix is through 'Intermatrix synthesis' (IMS) approach. This technique is based on loading of MNP precursors which could be metal ions or complexes, followed by chemical reduction using appropriate reducing agent to produce the desired zero-valent metal nanoparticle. Prior to precursor loading, the membrane surface should be functionalized so as to have appropriate functional group to hold the precursor. The use of functionalized polymer membrane as a support and stabilizing agent enables to synthesise nanocatalysts at the desired 'point use' and will result in formation of catalytically active polymer membrane. Encapsulation of MNPs in polymers membranes offer also unique possibilities for enhancing accessibility of catalytic sites to reactants [6, 7].

Among different successful membrane modification techniques, UV-induced grafting has been widely used because of its simplicity, mild reaction conditions, low cost, selectivity to absorb UV light without affecting the bulk polymer, and possibility of easy incorporation into the end stages of a membrane manufacturing process[8, 9]. We functionalized lab-made flat sheet and commercial hollow fibre polyethersulfone (PES) microfiltration membrane via UV induced graft polymerization of acrylic acid monomer (AA). Clélia Emin et al. [10], in the same research group, has successfully produced porous and nearly a dense poly(acrylic acid) grafted layer on hollow fiber commercial PES microfiltration membrane by varying different experimental parameters (monomer concentration and grafting experimental conditions). Based on this achievement, this research focuses on developing and testing catalytic

membrane reactors for liquid phase reaction based on porous grafted layers and gas/liquid contacting based on dense grafted layer.

Palladium (Pd) nanoparticles have been intensively studying for variety of catalytic applications such as hydrogenations, oxidations, C- C coupling reactions and electrochemical reactions in fuel cells[11]. Microporous polymeric membrane materials are ideal hosts for Pd-MNPs because of the higher surface area can provide a space for immobilization. Unique properties of supported Pd nanoparticles to absorb large quantities of hydrogen made them ideal catalyst for a number of hydrogenation reactions. 'IMS' of Pd nanoparticles supported on functionalized PES membrane is very efficient way to use its catalytic activity of surface atoms. In these experiments, both flat sheet and hollow fiber PES membranes were modified with poly(acrylic acid) photo grafting polymerization, subsequently, Pd-NPs were synthesized inside surface functionalized membranes via 'in situ' reduction of metal precursors. These will have higher potential applications for treatment of polluted surface and underground water, as conventional microfiltration membranes are incapable of separating trace and toxic molecular pollutants by size exclusion.

1.1 Objectives of the research

The overall objectives of this research includes

    I.   Development of catalytic polymer membrane reactor for liquid phase reactions
    II.   Development of catalytic membrane reactors applicable for gas/ liquid contacting

To be more specific the research involves:

    I.   Surface modification of commercial hollow fiber and lab made flat sheet PES microfiltration membrane using UV-induced graft polymerization
    II.   Preparation of palladium nanoparticle via intermatrix synthesis inside functionalized membranes
    III.   Catalytic performance test and kinetic analysis of the membrane using reduction of nitrophenol as a model for liquid phase reaction (effect of concentration, and catalyst weight on both the conversion, rate constant)
    IV.   Application of Pd loaded catalytic membrane for hydrogenation of nitrophenol, as a model for gas/liquid contacting

2. Synthesis of Palladium Nanoparticles in Functionalized Polymer Membranes

2.1 Introduction

Nanomaterials (NMs), materials with at least one dimension less than 100 nm, possess different properties than its bulk (macroscopic) form. Such materials exhibit unusual features and superior properties based on quantum mechanics, which influence variety of material properties such as electrical, heat transfer, melting temperature, optical and magnetic properties [12, 13]. As a result, NMs form shape and size dependent chemical and physical properties that differ drastically from their bulk counterparts. In General, NMs are found to be advantageous owing to properties such as, (1) tunable/tailorable chemical, mechanical and physical properties associated with their fine size range (1- 100 nm) (2) enhanced activities related to their extremely large specific surface areas, which makes them advantageous for surface reactions like catalysis (3) high strength, toughness, and ductility (4) superior formability and potential plasticity and (5) reduced thermal conductivity [14, 15]. Taking advantage of these properties to develop new products and processes applied in wide range of applications, is believed to revolutionerize the industry.

Nanoparticles (NPs) are building blocks of nanotechnological applications. They are the starting point for many 'bottom-up' approaches for preparing nanostructured materials and devices. The size, shape, and surface morphology of nanoparticles are key parameters playing important roles in controlling the physical, chemical, optical, and electronic properties of these NMs [12].

As the size of NPs becomes smaller, the ratio of surface atoms to the atoms inside; becomes rapidly increasing and hence possesses higher surface area to volume ratio than their corresponding bulk state. The high surface energy of these particles makes them extremely reactive, and lead to aggregation without passivation of their surfaces via either steric or electrostatic hindrances. Some of the commonly used steric hindrances used for surface passivation to prevent unnecessary aggregation of NPs includes; protection by self-assembled monolayers such as thiol-functionalized organics; encapsulation in H_2O pools of reverse

microemulsions, dispersion in polymeric matrixes such as poly(vinylpyrrolidone) (PVP) or hyperbranched dendrimers [4, 13, 16].

Recently, research and development in NMs have been stimulated by their technological applications. In this regard, MNPs have shown special importance due to their potential applications in emerging areas of nanoscience and nanotechnology, such as catalysis, environmental remediation, sensing, and biomedical applications. The first technological applications of NMs were in catalysts [17]. Particularly, transition metal NPs are known for their catalytic application. Since industrial catalysts usually work on the surface of metals, MNPs which possess much larger surface area per unit volume than the bulk metal, have been considered as promising materials for catalysis. The large surface area to volume ratio increases the chemical activity. Hence, there are significant cost advantages in fabricating catalysts from nanomaterials. Use of MNPs for catalysis is therefore, the best strategy to efficiently utilized expensive metals. In spite of higher catalytic activities, application of is mainly limited by their insufficient stability arising from a tendency to self-aggregate and coalescence between individual units. Owing to their higher surface energy, NPs have higher degree of tendency to aggregate in solutions without proper stabilizing agents. As a result of aggregation, NPs loses their catalytic activity[14]. Various stabilizing agents such as ligands, polymers or ionic liquids are used to prevent MNP's aggregation by steric, electrostatic or a combination of both effects.

The synthesis of stabilized, uniform and nanometer sized MNPs have been an intensive research for many years. It is worthy to mention here; Vladimir P. and his coworkers [4] for detailed review on synthesis and characterization of monodisperse MNP Catalysts. Synthesis of NPs can be carried out through various synthesis pathways based on either 'bottom-up' or 'top-down' approaches. Most often, the synthesis of MNPs involves the use of stabilizing agents or surfactants, which helps to prevent NPs aggregation and Ostwald ripening. In such cases, stabilizers not only preserve NPs size but also play a crucial role in controlling the shape.

NPs can be prepared by two different approaches, namely, 'in situ' and 'ex situ' techniques. In the first case, NPs are grown and synthesized by chemical reduction of metallic precursors inside a matrix, yielding a material that can be directly used for different applications. Whereas, in the 'ex situ' approach, NPs are pre-synthesized in a phase different from their

final application. They are first produced by soft-chemistry routes and then transferred and dispersed in a liquid or solid media[18]. However, the success of such approaches for dispersing the NPs is limited by their re-aggregation. This is the most common problem for many NPs prepared using 'ex-situ' fabrication techniques[19]. Because of their preferential advantages, 'in situ' synthesis approaches are currently the focus of research. Such approaches allow the preparation of a variety of metal-polymer matrix nanocomposites with highly controllable particle size and material morphology. One of the most promising routes to produce the polymer stabilized/supported MNPs and nanocomposites is based Intermatrix Synthesis (IMS), which consists of sequential loading of the functional groups of the polymer with desired metal ions (MNP precursors), followed by their chemical reduction.

Stabilization and immobilization of MNPs on solid support, besides to maintaining catalytic activities for long period by preventing aggregation, it offers an option to provide mechanical support.The application of polymer membrane as a support and stabilization media for MNPs synthesis, via 'IMS' approach is advantageous from different perspectives. Firstly, the development of polymer membrane-stabilized MNPs is considered to be one of the most promising solutions to the issue of NPs stability, by preventing self-aggregation. Secondly, the incorporation of MNPs into polymeric membrane matrices endow the membrane with catalytic property. Thirdly, the use of immobilized NPs reduces the chances of their leakage to the environment.

A conventional strategy for colloidal synthesis is the reduction of metal precursors in polar solvents in the presence of surfactants that prevent nanoparticles from aggregating in solution. Alcohols usually play the roles of both solvents to dissolve metal precursors and reducing agents to generate metal nanoparticles, while polymers such as poly(vinylpyrrolidone) (PVP) or hyperbranched dendrimers can serve as stabilizing agents.
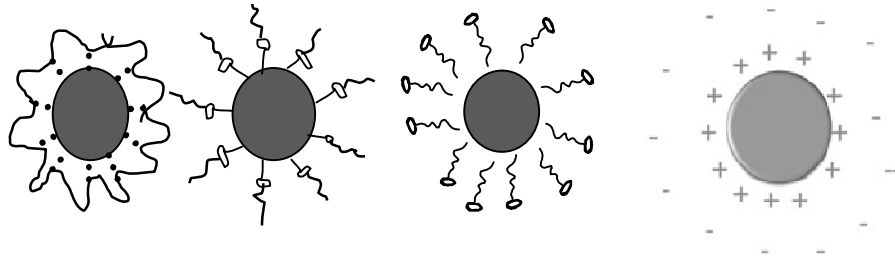
Figure 1. Stabilization of nanoparticles with steric (left, different short range polymers) and electrostatic hindrance (right)

2.1.1 Polymer Membrane Modifications

Surface functionalization of membranes is a techniques that can endow the membrane materials with desired properties. It has been widely applied to polymeric membranes in many fields and have progressed rapidly in recent years. To further increase the applications of the commercially existing polymeric membranes in different fields, the surface functionalization has become a key point in membrane science and technology. It can improve the performance of the established polymeric membranes either by minimizing undesired interactions such as, adsorption or adhesion; that reduce the performance through membrane fouling or by introducing additional interactions (affinity, responsiveness or catalytic properties) for entirely different applications [9].

Generally, some polymeric materials that have excellent physical and chemical properties often lack suitable surface properties required for specific applications. For this reason, surface modification of polymeric membranes has become prime importance in various applications from the advent of membrane-involving industries. It mainly offers a versatile means for improving the surface properties such as: hydrophilicity, hydrophobicity, biocompatibility, anti-fouling, surface roughness, conductivity and anti-bacterial properties, while preserving the bulk structure and property of the base membrane.

Polymer membrane functionalization can be carried out using different techniques such as surface chemistry, polymer deposition, alternate adsorption of oppositely charged

polyelectrolytes, and radiation induced grafting. It involves, introducing functional groups through covalent or non-covalent attachment mechanisms. Specially in radiation induced surface graft polymerization, the modification is achieved by 'tethering' suitable macro molecular chains on the membrane surface through covalent attachment. The availability of multitude of different grafting monomers to tailored the surface of the membrane to acquire distinctive properties makes it advantageous. It also ensures an easy and controllable introduction of tethered chains with a high density and exact localization onto the membrane surface. Compared with the physical modification methods such as coating, the covalent attachment of polymer chains onto the membrane surface avoids desorption and maintains the long-term chemical stability of the modified surface[8].

Among the different successful radiation induced membrane modification techniques, UV-induced grafting has been widely used because of its simplicity, mild reaction conditions, low cost, selectivity to absorb UV light without affecting the bulk polymer, and possibility of easy incorporation into the end stages of a membrane manufacturing process[8, 9].

During the past years, polyethersulfone (PES) had been extensively utilized in microfiltration and ultrafiltration membranes due to its good thermal stability, chemical resistance, excellent processability, and easy in controlling its porosity and morphology[20]. Currently, modification of PES to endow new properties (fouling resistance, catalytic effect) is applied using UV- induced grafting. The mechanism of photochemical grafting involves, when a chromophore on a macromolecule absorbs light, it becomes energetically excited and dissociated into reactive free radicals, that can initiates grafting process. If the formation of free-radical sites is not possible by the absorption of light, addition of photoinitiator is necessary. Sensitive polymer membranes can generate free radicals without photoinitiator which on the backbone of the polymer, and this free radicals react with monomers to form the grafted polymer. However when a photoinitiator is used, upon exposure to UV light, the photoinitiator forms free radicals that can undergo diffusion and attached to the hydrogen atoms in the support, producing the radical sites required for grafting[1, 8, 20].
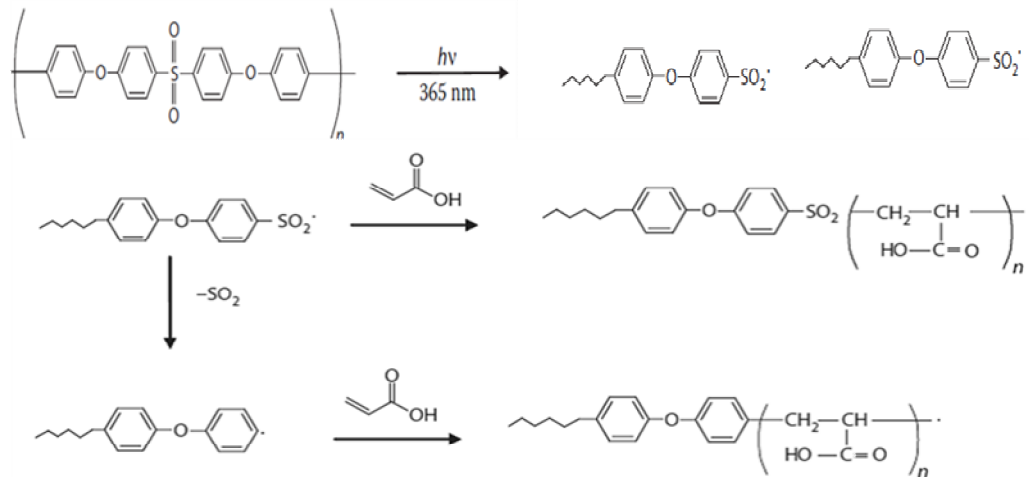
Figure 2.The mechanism of photochemical modification of PES with AA[1].

2.1.2 Intermatrix synthesis (IMS) of metal nanoparticles

Several publications on MNP synthesis described IMS as the most favorable synthesis method for catalytic application, as it is possible to immobilize the NPs near the surface[21]. MNPs with desired composition, size and structure can be synthesized by controlling parameters like polymer matrix type, type of the functional groups, and metal reduction conditions. The type of functional groups of the polymer (can be cationic or anionic) determine the type of MNPs precursor and the sequence of IMS stages. MNP synthesis based on IMS involves two consecutives stages: a) the loading of the functional groups of the polymer with metal precursors followed by b) their reduction inside the matrix resulting in the formation of monometallic MNPs. Reduction can be carried out by using $NaBH_4$ or other reducing agents[18].

(1) Functionalized membrane

(2) Precursor loading

(3) Reduction with NaBH$_4$
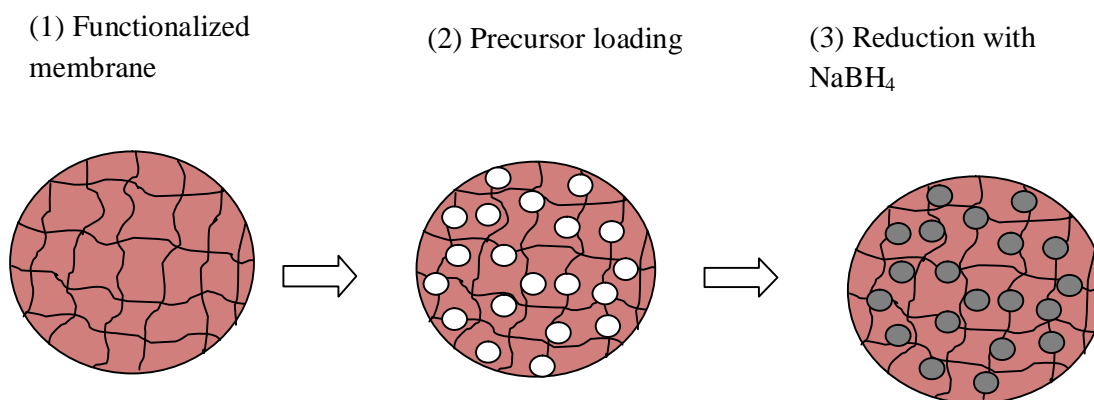
Figure 3. Intermatrix synthesis NPs on functionalized polymer membrane support

2.2 Experimental

2.2.1 Materials and Methods
Materials

The following chemicals and materials were used during the experiment. acrylic acid (AA), N-methyl-2-pyrrolidone (NMP), polyvinylpyrrolidone powder (PVP, M$_w$ =29,000), casting knife, acrylic acid (AA), N, N`-methylene-bisacrylamide, 4-hydroxybenzophenone, tetra-ammine palladium(II)chloride monohydrate. All compounds have been used without any purification and solutions were prepared with deionized water.

2.2.2 Membrane Preparation
Flat sheet PES-MF membranes were prepared via unsteady state phase inversion method using a solution containing polyethersulfone (18% wt) as polymer and N-methyl-2-pyrrolidone (62% wt) as solvent, and polyvinylpyrrolidone(PVP 20 %wt) as a pore former. The solution was casted using a casting knife with 350 μm thickness and is precipitated in a coagulation water bath at 18-20 ℃.
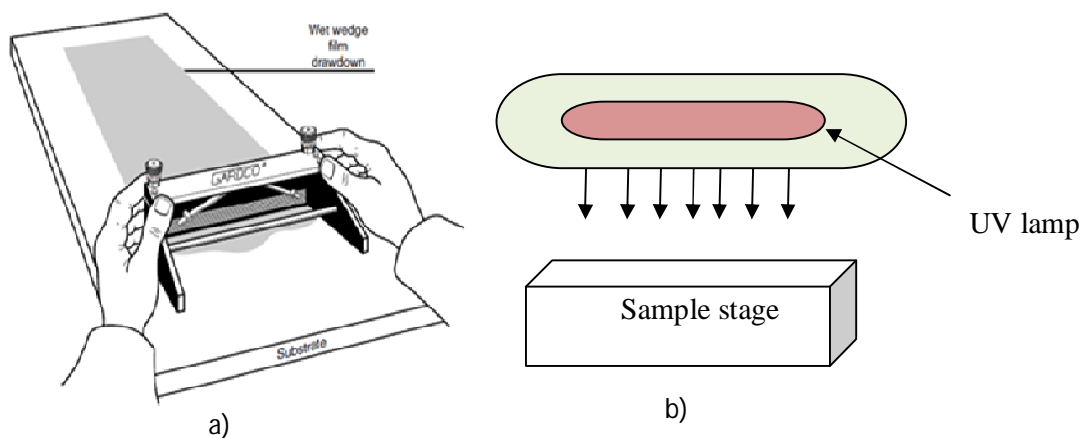
Figure 4. a) Casting knife for PES MF membrane and b) Set-up for batch UV irradiation for grafting.

2.2.3 Membrane Functionalization

Flat sheet PES microfiltration membranes were immersed for 3 minutes in 30 ml aqueous solution of AA monomer (25 wt %). After the immersion, samples were grafted using a simple photografting setup, containing quartz UV lamp. Exposure time was (5-20) minutes. Distance from the light source to the sample was adjusted to a minimum 6 cm, in order to avoid a possible heat up of the membrane. After grafting, samples were washed with deionized water in order to remove unreacted monomer. Dried samples were taken for surface analysis surface using attenuated total reflection fourier transform infrared spectroscopy (ATR-FTIR, Thermo-Nicolet Nexus)

2.2.4 Precursor loading and intermatrix synthesis of Pd nanoparticles

The synthesis of Pd-NPs inside the functionalized flat sheet PES polymer membrane matrix was carried out via Intermatrix synthesis method with procedures consisting of: (1) Palladium salt [Pd(NH$_3$)$_4$Cl$_2$] was loading to the functionalized membrane which enables cation exchange between carboxylic groups of functionalized PES with [Pd(NH$_3$)$_4$]$^{2+}$ ions to took place and (2) subsequent chemical reduction by 0.1M NaBH$_4$ solution: The cation exchange was performed by submerging grafted membrane in to palladium precursor solution (0.01 M Pd(NH$_3$)$_4$Cl$_2$) over night at room temperature. The synthesis can be summarized by the following sequential equations of ion exchange (1 & 2) and chemical reduction (3&4)[6].

$$2R–COO^-H^+ + [Pd(NH_3)_4]^{2+} \rightarrow (R\text{-}COO^-)_2[Pd(NH_3)_4]^{2+} + 2H^+ \text{--------------(1)}$$

$(R-COO^-)_2[Pd(NH_3)_4] + 2Na^+ \rightarrow 2(R-COO^-)Na+ [Pd(NH_3)_4]^{2+}$----------------(2)

$[Pd(NH_3)_4]^{2+} +2BH_4^- + 6H_2O \rightarrow Pd^0 + 7H_2+ 2B(OH)_3+ 4NH_3$----------------(3)

$[Pd(NH_3)_4]^{2+}+ 2e^- \rightarrow Pd^0 + 4NH_3$------------------------(4)
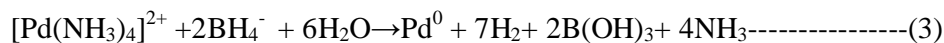
Palladium Content measurement

The amount of palladium loaded to the functionalized membrane was determined by using inductively coupled plasma optical emission spectrometry (ICP-OES, Ultima 2, Horoba Jobin Yvon). 1 cm^2 sample of Pd loaded membrane was dissolved in aqua regia; which is a highly corrosive mixture of acids, for two days. The acid mixture was prepared by freshly mixing concentrated nitric acid (65 %) and hydrochloric acid (35%) in a volume ratio of 1:3. It was then diluted in ultra pure water so as to analyze in ICP.

2.3 Results and Discussion

ATR- FTIR Results

Both unmodified PES and the UV- induced modified flat sheet membranes were characterized by ATR-FTIR. Fig.3, shows the spectra of the unmodified and modified membranes with AA monomer. As can be seen; UV- induced grafted membranes exhibit different ATR-FTIR spectra than the unmodified one. In addition to the typical PES bands of the unmodified membrane, the IR spectra of modified membrane show additional peak at 1720 cm^{-1}, which corresponds to the carbonyl (C=O) group bands of COOH, which indicates the existence of poly(acrylic acid) chains[20] and assured that the monomer is successfully polymerized on the substrate PES. Also, with UV modification, some original absorbance peak intensity is decreased that can be contributed to increase coverage of the PES surface by poly (acrylic acid).
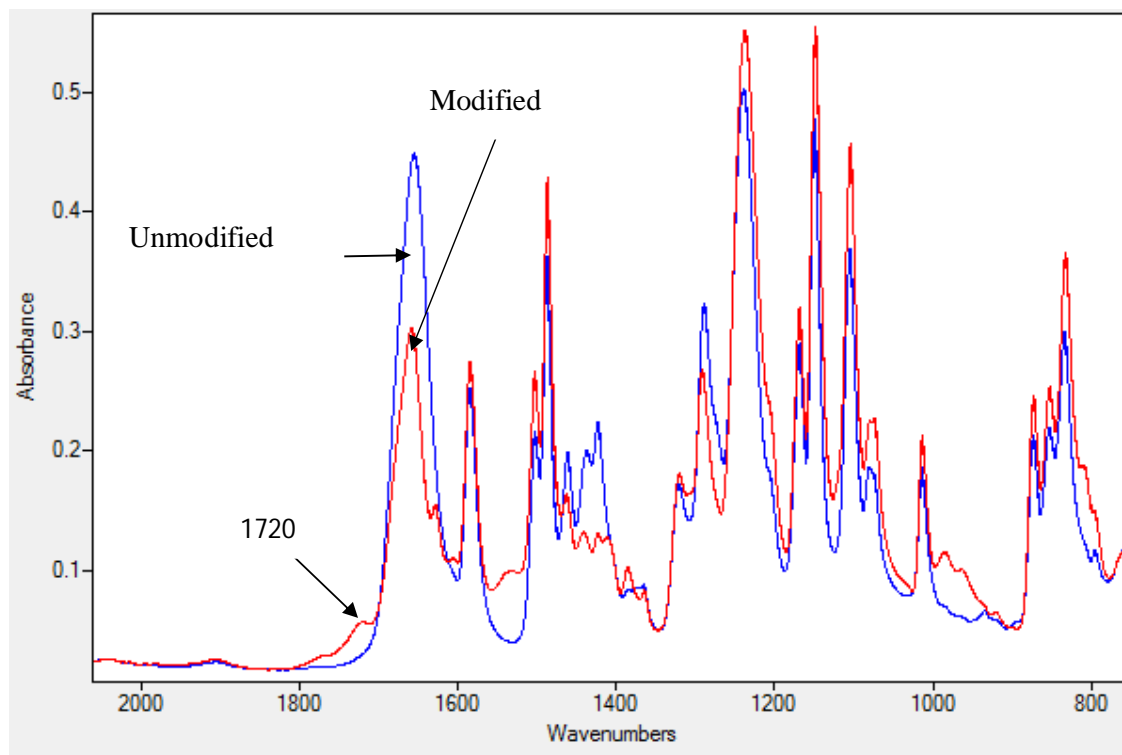
Figure 5. The ATR-FTIR spectra of the unmodified PES flat sheet membrane and modified membranes using UV grafting of AA (25 wt %) at 20 min UV batch irradiation time.

Apart from this, as can be seen from FTIR spectra of modified membrane in Fig.6 ，the intensity of the new peak at 1720 cm^{-1} increases with photografting reaction time which corresponds to the energy received during graft polymerization. The more energy received by the monomer, the higher degree of modification. In addition to the new absorption peak corresponding to the carbonyl group (C=O) of COOH, there are also other new small absorbance peaks appeared at 1625,1605 and 1535 cm^{-1} for the modified membranes. The small absorbance peak for the AA-modified membranes at these regions attributed to the presence of additives such as PVP in the original casting solution and cross linker in the monomer solution; as reported by Ahmad R.[22] and Roy B. et al.[23]   Also, the disappearance original peaks at 1640–1680 cm^{-1} for the modified membranes indicates that the modification was successfully.

13
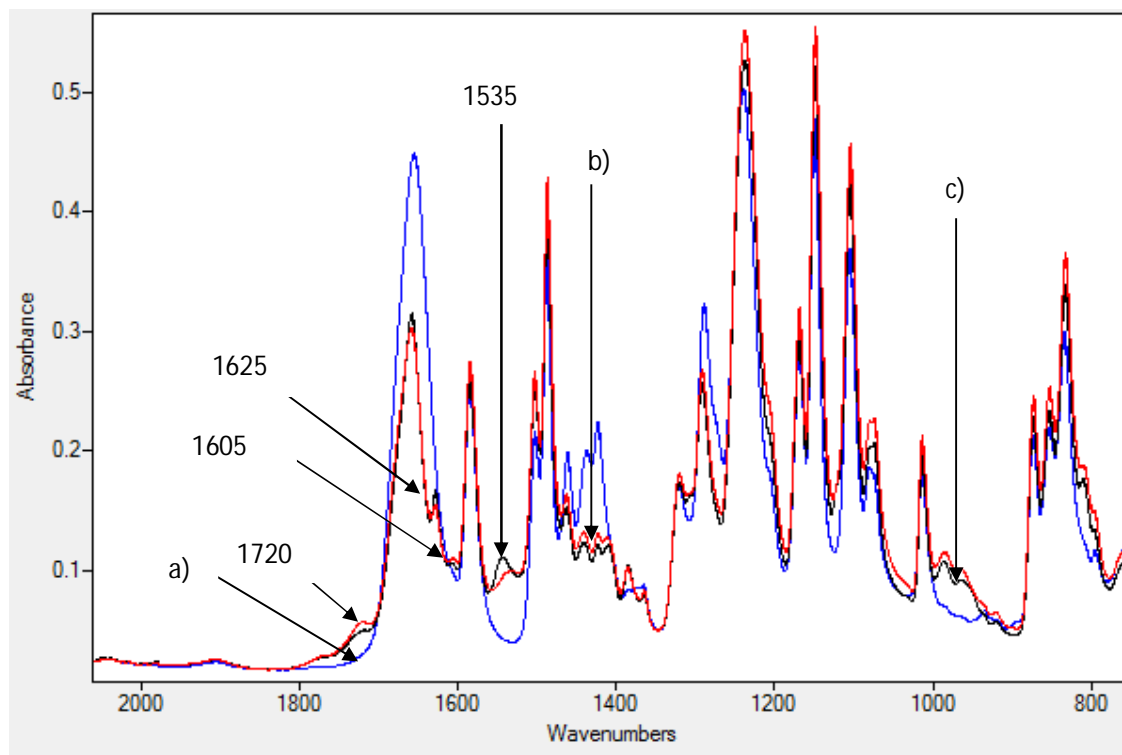
Figure 6. The ATR-FTIR spectra of the a) unmodified flat sheet PES membrane and modified membranes using UV induced grafting with (25 wt % AA); b) 20 and; c) 15 minute UV irradiation time respectively.

The white flat sheet membrane turned immediately to grey color after Pd reduction by sodium borohydride, which was a good qualitative indication for the formation of Pd nanoparticle[24]. Membranes grafted at different times were used to synthesized Pd nanoparticle. ICP analysis showed that the weight of Pd loading is increasing with grafting time (energy received). These data are in agreement with expected and FTIR results. At higher energy, the intensity of the modified functional group was stronger which can lead to better cation exchange with Pd precursor and thus, higher Pd amount from the reduction.
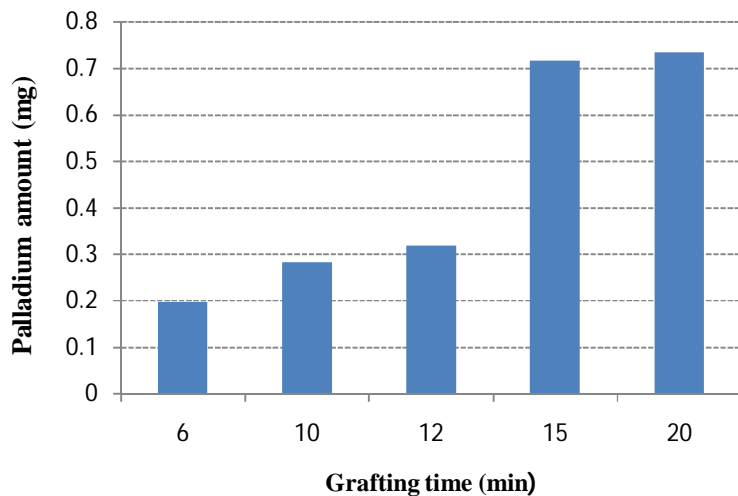
Figure 7. Palladium amount per membrane (15.2 cm^2) versus grafting time

In summary, both the SEM images and IR spectrum showed that the monomer is successfully grafted which is assured by the new formation of COOH group. Hence the COOH group of the modified membrane can undergo ion exchange with Pd salt precursor, which is a prerequisite for intermatrix NP synthesis.

15

3. Catalytic Polymer Membranes for Liquid Phase Reactions

3.1 Introduction

A membrane reactor (MR) is a bifunctional device combining a membrane-based separation with catalytic chemical reaction in one device. MR becomes one of the approaches for process integration, which promises numerous benefits in accordance with the strategy of process intensification, that can improve the yield or reaction selectivity and decrease downstream separation[3]. In the recent years, many approaches have been proposed to combine membrane properties with chemical reaction in order to intensify a process. These includes, extractor type, distributor and contactor type. Depending on the type of membrane reactors, the membrane performs different functions [25, 26]

1. 'Extractor'- applied to selectively remove the products from the reaction mixture,
2. 'Distributor' - used to control the addition of reactants to the reaction mixture
3. 'Contactor'- provide an interfacial contact area for reacting streams and intensify the contact between reactants and catalyst

The membranes integrated with reaction can be either noncatalytic (inert type) or catalytic-membranes that have catalysts incorporated in their porous structure or on the surfaces. In MRs, the position of membrane layout could be either inside the reactor forming 'in situ separation unit' or physically two distinct units with the reactor forming 'ex situ separation unit'[27].

Extractor membrane reactors

Majority of MRs belong to this category, in which one of the product is continuously and selectively removed from the reaction mixture by the membrane. If the reaction is limited by the thermodynamic equilibrium, the conversion can be increased by removing one of the product component, so that the equilibrium shifts towards the desired product side[28]. If the reaction rate of the undesired secondary reaction is higher than that of the primary reaction, the reaction selectivity can be significantly enhanced by removing the desired intermediate species. Particularly, the advantage of selectively removing the valuable product lies in avoiding further separation steps or reducing the separation units by increased product concentrations. Furthermore, if one of the product has inhibition effect, as in case of some fermentations, removing this product strongly improves the reactor productivity[29].

A driving force for permeation is created by lowering the partial pressure of permeate component than that on the feed side pressure. This can be achieved by applying a difference

in absolute pressure, by dilution of the permeate with an inert component or by applying a reactive sweep gas. The most frequently used applications of extractor membrane reactors are in catalytic dehydrogenations of light alkanes used for hydrogen generation, such as steam reforming reactions. It is worthy to mention Dittmeyer et al.[28] for their clear review on the application of different Pd-based membranes for dehydrogenation reactions. Applications for esterification reactions have also been reported [30].

Distributor membrane reactors

In this type of MR, one of the reactant is specifically added to the reaction mixture across a membrane. The membrane can act as; even distributor of the limiting reactant along the reactor to prevent side reactions and as upstream separation unit to selectively dosing one component from a mixture. Controlled addition of oxygen in gas-phase partial oxidation of hydrocarbons in which the intermediate product reacts more intensively with oxygen than the reactants, in order to prevent total oxidation[31, 32] are the main application of this category of membrane reactor.

Contactor Membrane reactors

In this configuration, the reacting species are feed at different sides of the membrane and must diffuse through the catalytic layer to react. Therefore, the role of the membrane is to provide an interfacial contact area for the reacting streams, but does not perform any selective separation. The two sides of membranes are used to bring reactants into contact and if the reaction rate is fast compared to the diffusion rates of the reactants, the reaction occurs in the catalytic layer in a way that prevents mixing of reactants. Due to higher surface area of membranes, a contactor mode can provide higher contact area between two different phases. Specially, if one phase has lower solubility in the other phase, higher surface area contact between these phases can decrease the need of higher pressure that could have been applied for lower soluble component. Gas/liquid contactors and flow-through membrane reactors are important class of membrane contactors.

3.2 Flow-Through Catalytic Membrane Reactor (FTCMR)

In this kind of membrane reactor configuration; unselective porous catalytic membrane, either inherently catalytic or made catalytic by impregnation of nanocatalysts, is applied in dead-end mode operation. The premixed reactants are forced to pass through the catalytic membrane. The function of the membrane is to create a reaction environment by intensive contact between the reactants and catalyst with short and controlled residence times, and high catalytic activity. The main drawback in classical fixed-bed reactors is that, the desired conversion is mainly limited by the pore diffusion. However, if reactants can flow convectively through the catalyst sites, the resulting intensive contact between reactants and catalyst can result in a high catalytic activity[33, 34]. Besides, this can avoid the problems derived from internal or external mass transfer resistance that may appear in a conventional fixed bed reactor. In FTCMR, the reactants flow convectively through the membrane to catalyst sites, which in turn results in an intensive contact between the reactants and the catalyst, thereby leading to higher catalytic activity with negligible mass transport resistance. Furthermore, the introduction of convective flow can avoid undesired side reactions [2, 34]. In the case where the catalyst is placed inside the pores, the number of collisions between the reactants and catalytic sites inside the pores can be amplified noticeably by decreasing the pore diameters to small values, so that Knudsen diffusion becomes predominant. The combination of Knudsen diffusion with the FTCMR configuration is believed to result in a feature that enable reactant molecules to have multiple contacts with catalyst surface [26, 35].

The main technological reasons to apply FTCMR are aimed at: (1) achieving complete conversion at minimum time or space, by taking the advantage of high catalytic efficiency, (2) obtain maximum selectivity for a given reaction because of narrow contact time distribution. Depending on the rate of chemical reaction, the reactants can pass through the catalytic membrane with a single pass; or are allowed to multiple pass and circulated in membrane loop module and a feed tank for higher conversion[25].

To date, many publications are reported in literature for potential applications of FTCMR for both gas and liquid phase reactions. To mention some, it is applied in volatile organic compound destruction [36], gas phase photocatalytic oxidation [37], partial oxidation reactions [38], partial hydrogenation [39], oxidative coupling and oligomerization reactions

18

[40] and hydrogenation of nitrate in water [41]. Almost all literatures dealing with flow through catalytic membrane reactors studied time behavior of reactions in multiple pass operation and circulation of reactants or taking the pores of the membrane as microreactors, so as to assume as ideal batch reactor. As the reaction mixture is brought in to contact with the catalytic membrane by applying pressure in the feed tank, taking in to account the applied pressure (convective flow) is important. A detailed review of FTCMRs and their applications; can be found elsewhere in literature [26].

In FTCMR, functionalized porous membranes are used instead of dense membranes. The advantage of this type of membrane lies in their small mass transfer resistance compared to their dense counterparts. However this is also their drawback, since the flow is mainly convective through the membrane pores, the separation properties of the polymeric membrane are not used and the membrane acts basically as catalyst support.

Recently; polymeric membrane reactors are developed via surface functionalization and catalyst immobilization on commercial microfiltration membranes. Shah T.N. and coworkers [42], has developed catalytically active membranes by grafting sulfonated polystyrene chains on the commercial PES microfiltration membrane substrate and applied for the esterification reaction of ethanol and acetic acid. The grafted sulfonated polystyrene chains on the surface of the membrane, which are accessible to the reactive species; have been demonstrated as strong heterogeneous acid catalysts. On the other hand, synthesizing and immobilizing of metal nanoparticles inside the pore walls of polyvinylidene fluoride (PVDF) microfiltration membrane functionalized with poly (acrylic acid) (PAA), has also been reported[43]. The experiment was aimed at using the pores as catalytic micro channels, where functionalization was done by 'in situ' free radical polymerization of acrylic acid in the microfiltration membrane pores.

Nevertheless, in a conventional batch reactor where the catalyst particles are suspended, the reaction rates are quite low because of the immiscibility of the organic and aqueous phases which leads to a much lower concentration of one of the reactants in the other one phase. In such a reactor, the use of a co-solvent is required to increase the organic reactant concentration at the catalyst surface and therefore increase the reaction rate. Using a co-solvent at the industrial scale represents however serious technical and environmental limitations for this chemical process.

19

When reactions are performed in a conventional gas-liquid-solid slurry system, further separation is also needed for catalyst recovery. The contact time and the reaction temperature are relatively difficult to control in the semi-batch slurry reactor for the exothermic reaction

Mathematical Model for FTCMR

Convective mass transport is taking place in FTCMR; because there exists transmembrane pressure difference between the two sides of membrane, so as to enforce the reactants to pass through. In some membranes, such as nanofiltration membrane, the presence of convective flow by pressure difference enhances the diffusive driving force. Hence investigating combined effect of the diffusive and convective flows is important in surface functionalized polymer membranes. The model takes in to account of simultaneous transport by convective and diffusive mass flow with chemical reaction. Clélia Emin et al. [10], has clearly shown that palladium nanoparticles have been only immobilized on the grafted poly (acrylic acid) layer. Analyzing the sample using energy-dispersive X-ray spectroscopy (EDX) showed, NPs were not found deep in the support membrane. This fact is considered here in modeling FTCMR. The following assumptions are considered for the first case (diffusion + convective) transport.

- Reaction occurs uniformly at every positions within the catalyst layer.
- transport of reactants through the catalyst layer occurs both by diffusion and convection. Here the assumption is, even if the diffusion is small compared to the convective term, due to continuous reaction across the catalytic layer which forms concentration gradient, molecules diffuse to the catalytic layer. However the diffusion term does not contribute much to permeate flow rate.
- Chemical reaction occurs on the interface of the catalytic particles so that, the diffusion inside the dens nanoparticle is negligible.
- There is no mass transfer resistance on both feed and permeate sides of the membrane
- The concentration changes only across the catalytic membrane layer and nanoparticles are immobilized and stabilized on the grafted layer.
- Single pass of reactant is considered
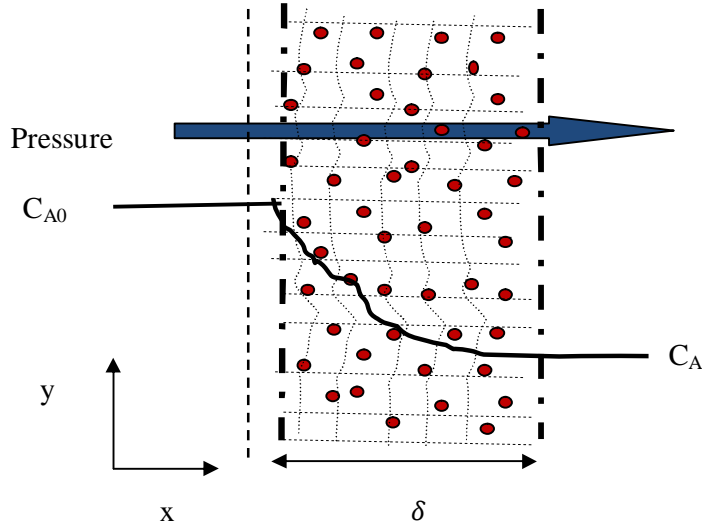
Figure 8. scheme of one dimensional mass transport across catalytic layer in flow through membrane reactor

If a one dimensional mass balance over the catalytic membrane layer is taken by considering both diffusion and convection, second order differential equation can be obtained. For pseudo first order reaction, $r_A = K_{app} * C_A$ (Look the detailed derivation in the appendix)

$$D\frac{d^2 C_A}{dx^2} - V_x \frac{dC_A}{dx} - K_{app} C_A = 0$$

Introducing dimensionless length $\varepsilon = x/\delta$, where δ is catalytic membrane layer.

$$\frac{d^2 C_A}{d\varepsilon^2} - P_e \frac{dC_A}{d\varepsilon} - \emptyset^2 C_A = 0$$

Solving the second order ordinary equation gives

$$\frac{C_A}{C_{A0}} = \exp\left[\frac{Pe\ \varepsilon}{2}\right]\left[\frac{Sinh(\varphi(1-\varepsilon))*\frac{Pe}{2} + \varphi\ \cosh[\varphi(1-\varepsilon)]}{\frac{Pe}{2}Sinh\varphi + \varphi cosh\varphi}\right] \qquad (3.1)$$

Where, $\varphi = \sqrt{\left(\frac{Pe^2}{4} + \emptyset^2\right)}$, $\emptyset^2 = \frac{K_{app}\delta^2}{D}$, and $P_e = \frac{V*\delta}{D}$

we can predict the concentration distribution at the end of the membrane ($\varepsilon = 1$), as function of initial concentration, peclet number and reaction modules $\emptyset$ with the following equation.

$$\frac{C_A}{C_{A0}} = \frac{\varphi * \exp\left[\frac{Pe}{2}\right]}{\frac{Pe}{2} Sinh\varphi + \varphi cosh\varphi} \qquad (3.2)$$

However, if we don't take in to account the diffusion (the diffusion is negligible, as the system is convective dominant), the above equation becomes

$$C_A = C_0 \exp\left[\frac{K_{app}\delta}{J_v}\right] \qquad (3.3)$$

where J_v is the flux in (m^3 h^{-1}m^{-2}) or convective velocity in (m/h) (Look the detailed derivation in the appendix)

3. 2. Experimental

Catalytic performance Test

The catalytic performance of Pd loaded flat sheet PES membrane was evaluated by the reduction of *p*-nitrophenol to *p*-aminophenol with NaBH$_4$ in a flow through reactor. The reduction is depicted in the following figure. This reaction is catalyzed by free or immobilized nanoparticles and proceeds in aqueous solution at ambient temperature. Moreover, it can be easily monitored via UV-visible spectroscopy by the decrease of the strong adsorption of 4-nitrophenolate anion at400 nm.

The reduction of NP in the presence of nanoparticles has been frequently used previously in order to evaluate the catalytic activity of different metal nanoparticles immobilized on membranes[10, 24, 44]. In addition, this reaction has been used to test the catalytic activity of metal nanoparticles immobilized in other carrier systems like core-shell. Previous work demonstrated that NP is reduced to aminophenol is only possible in the presence of the catalyst; no reaction takes place in the absence of the nanoparticles[24]. In flow through membrane reactor configuration, a solution containing different concentrations of a mixture of *p*-nitrophenol and NaBH4, was forced to cross the membrane. An excess of NaBH$_4$ was used, so that the kinetics can be assimilated to a pseudo first order in terms of concentration of *p*-nitrophenol. The progress of the reaction was monitored by measuring the concentration of p-nitrophenol using UV–visible spectroscopy at (λ= 400nm).

22
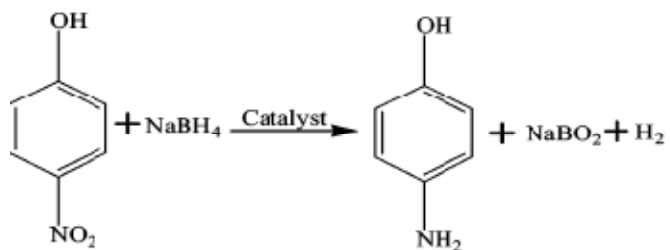
Figure 9. Schematic for reduction of p-Nitrophenol to p-Aminophenol with $NaBH_4$ [45]
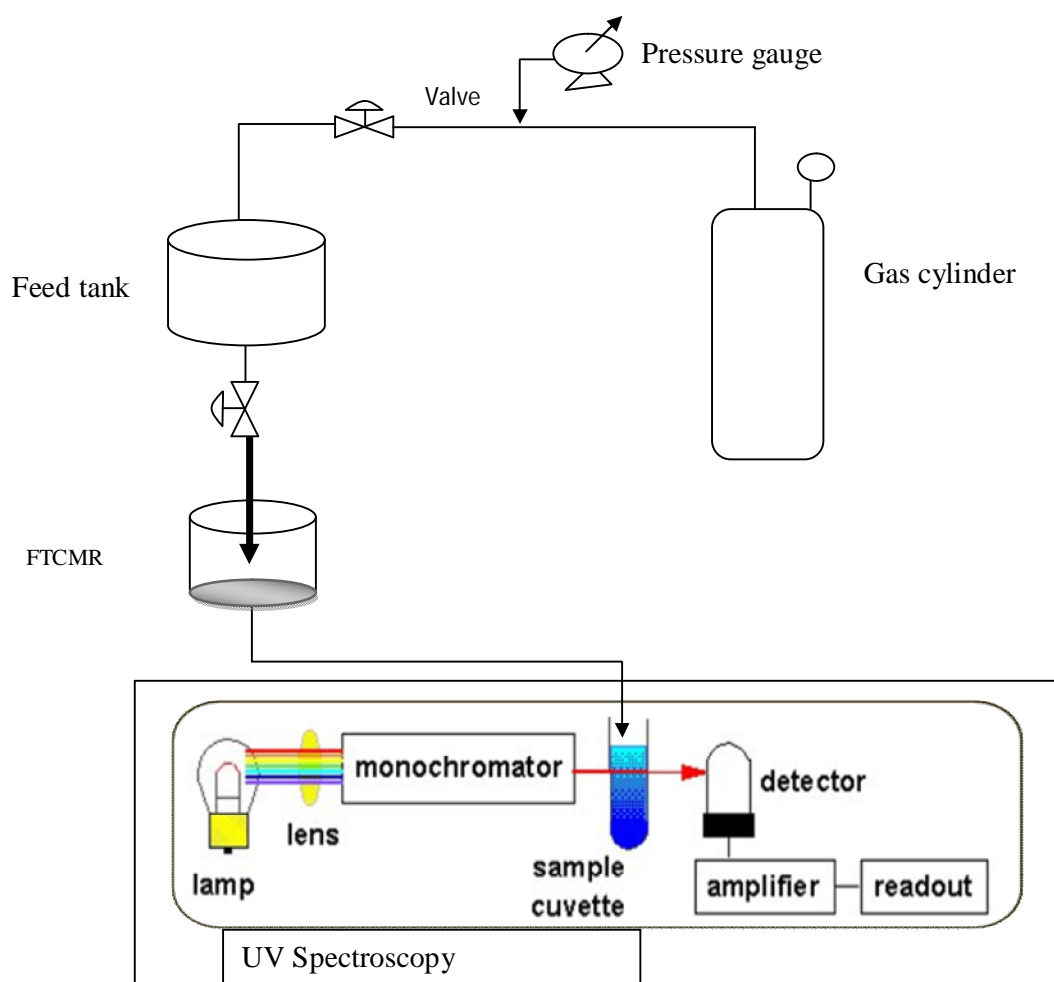
Figure 10. FTCMR Experimental Setup

UV-visible spectrometry measurement

The precursor solution of nitrophenol in sodium borohydride shows an intensive yellow color. This allows for concentration measurement by means of UV-visible spectrometry. The catalytic conversion of nitrophenol has a light absorption peak at a wavelength of 400 nm and was measured by means of a Biochrom Libra S12 UV-Visible spectrophotometer. Samples of the precursor solution was analyzed before the reaction to determine the initial absorbtion of the reactant and after each reaction step. The absorbance of NP is proportional to its concentration according to the Lambert-Beer equation; as a result, the absorbance can be used in the rate expression instead of concentration.

$A = \varepsilon C l$ [1], where (A = absorbance at a time ; ε = molar extinction coefficient; l= length of the light path through the sample (cuvette length) and , C = sample concentration). From the above proportionality

$\dfrac{A}{A_0} = \dfrac{C}{C_0}$; where A_0 is absorbance of the initial concentration, C_0. For batch reactor

$C = C_0 exp[-K_{app}t]$

$$ln\left(\dfrac{A}{A_0}\right) = -K_{app}t \tag{3.4}$$

The apparent rate constant K_{app} is determined by the slope of the curve obtained by $ln(A/A_0)$ as a function of time. In order to account the Pd catalyst, a new intrinsic reaction rate constant, k, was introduced by further normalizing K_{app} with Pd content.

$$k = \dfrac{K_{app}}{m}$$

where *m* is the dosage of Pd per 15.2 cm^2 of membrane.

Flow through reactor as "Packed Bed reactor"

To consider the effect of catalyst weight, the flat sheet membranes were grafted at different grafting times; hence different grafting layer and different amount of Pd loading. These membranes were used to test nitrophenol reduction in dead end configuration mode. In such cases, each membrane can be assumed as thin layer 'packed bed' of catalysts without pressure

---

[1] Lambert-Beer equation

drop. Other conditions were kept the same. As, the membrane had not rejection for nitrophenol, a mass balance with no accumulation over the grafted layer was taken;
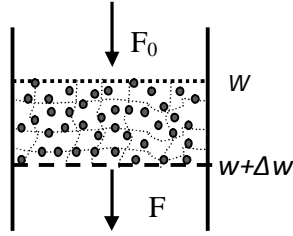
Figure 11. Schematic representation of flow through reactor as packed bed reactor

Mass balance across the catalytic layer packed with catalysts gives

Fw - F(w+Δw) + r = 0 , where r; is rate of reaction in terms of catalyst weight, F_0 and F are inlet flow and outlet flow rates (mol/sec) respectively, w is weight of catalyst. For nitrophenol, the above general equation gives a differential equation of

$$\frac{dF}{dw} = -K_{app}C, \quad \text{, where F} = Jv*C*A m$$

$$J_v A_m \frac{dC}{dw} = -K_{app}C,$$

$$C = C_0 exp\left[-\frac{K_{app}w}{J_v A_m}\right],$$

Where K_{app} is the apparent pseudo-first-order rate constant; J_v is flux and A_m is membrane area and; w is weight of catalyst. Conversion in terms of catalyst is then given as;

$$X = 1 - \frac{C}{C_0}$$

$$X = 1 - exp\left[-\frac{K_{app}w}{J_v A_m}\right] \tag{3.5}$$

where C and C_0 are outlet and inlet concentrations respectively.

Batch Reactor Mode

Batch experiments were carried out in 200 ml glass at atmospheric conditions. The $NaBH_4$, was taken in excess for a reasonable assumption of pseudo first order reaction (typically 20:1 mole ratio) with respect to nitrophenol. The time at which the catalyst containing membrane was added to the mixture was considered as zero-time. To achieve better contact, the Pd

containing flat sheet membrane (15.2 cm^2) was cut into pieces and added to the reacting mixture. As the use of mechanical agitation could have been detach the Pd nanoparticles, the reactors were agitated using compact flat orbital shaker (IKA$^®$ KS 260 basic) to minimize external mass transfer resistance. The catalytic activity of the membrane was compared with FTCMR by performing the reaction under the identical conditions and equivalent Pd catalyst amount. Initial samples were withdrawn frequently to characterize any short-term change inactivity. Samples were also collected at longer times to characterize the stability of the catalytic membrane and to check the conversion. All catalytic tests were performed at least twice in order to ensure reproducible results. The governing equation for conversion in batch reactor conversation can be given by

$$\frac{dC_N}{dt} = -r,$$

where r is the reaction rate and C_N is nitrophenol concentration

$$\frac{dC_N}{dt} = -K_{app}C_N$$

$$C_N = C_0 exp[-K_{app}t]$$

where C_0 is initial concentration and $Kapp$ is apparent pseudo first order kinetic constant

$$X = 1 - exp[-K_{app}t] \tag{3.6}$$

3.2.2 Results and Discussion

Batch Vs. Flow through reactor

Nitrophenol (0.12 mM) reduction using aqueous NaBH$_4$ was performed in flow through reactor at 60 LMH and 0.318 mg of Pd catalyst. At the same, concentration and catalyst weight, the reduction was done using batch mode operation. Fig. 12 shows a comparative conversion of nitrophenol in flow through and batch mode of operation. As can be seen, the flow through mode out performs batch mode of operation. This improved kinetic performance of the flow through catalytic membrane is due to the fact that the transport of the reactants by convection greatly enhances reactant access to catalytic sites located in the membrane surface.

As a result, the behavior of the catalytic membrane in flow through reaction should resemble that of a homogeneous catalyst. Theoretically it was expected, the batch mode will have the same conversion starting from 100 minute. However, under this condition no progress has been observed after 140 minutes and the actual conversion after three days was even less than that of the flow through.
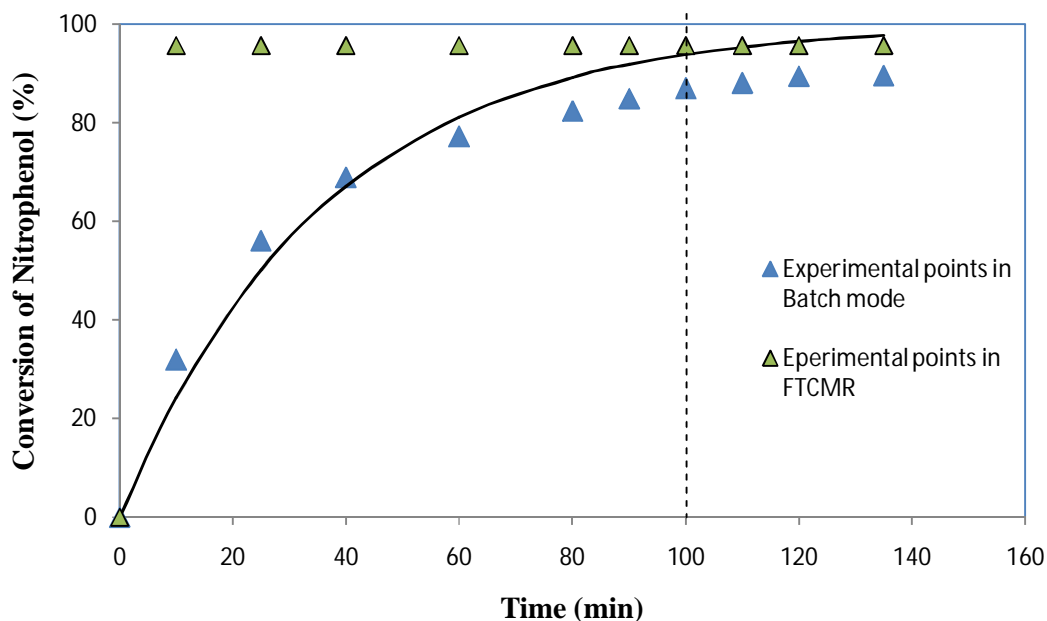
Figure 12. Conversion comparison in FTCMR and batch mode operation at the same initial concentration of nitrophenol (C_0 = 0.12 mM) and Pd weight of 0.318 mg a) 95.65% average conversion in flow through mode at 20 LMH, b) batch mode operation

It is well known that the rate of a chemical reaction depends on the concentration of reactants. Two different initial p-NP concentrations of 0.12 and 0.096 mM with 14.38 mM of NaBH$_4$ reductant were taken to study the effect of initial concentration on the catalytic reduction in batch operation, and the results are shown in Fig. 13. When *p*-NP concentration was increased, the apparent rate constant was observed to decrease. This phenomenon was unexpected, as increasing reactant concentration usually makes reaction fast. The same trend was also reported by many other authors [46-48]. This result can be explained by the reaction mechanism of nitrophenol reduction over Pd nanoparticle surface. Increasing concentration of *p*-NP leads to high percent coverage of the surface of the Pd nanoparticles with *p*-NP, which restricts the electron transfer from NaBH$_4$ to *p*-NP. This in turn slows down the reaction with

the borohydride ions and the injection of electrons to the metal surface. As a result of this, catalytic action of NaBH$_4$ is restrained. Besides, both mechanistic and experimental explanation showed that this reaction is based on Langmuir-Hinshelwood mechanism, where both reactants need to be adsorbed on the surface of the catalyst prior to reaction [46]. Hence, competitive absorption of the reactants results in slowing down the reaction. It is worthy here to state that Stefanie W. et al.[46] has investigated experimentally the mechanism of the reduction of NP by borohydride in the presence of metallic nanoparticles and has found the reaction is based on the mechanistic model of Langmuir-Hinshelwood. Accordingly, this catalytic reduction proceeds on the surface of the metal nanoparticles, in such a way that the nanoparticles react with the borohydride ions to form the metal hydride. Then when nitrophenol adsorbs onto the metal surface, the reduction takes place and they found that the rate-determining step is the reduction of the adsorbed nitrophenol to aminophenol. Our result is in agreement with these authors by the fact that, the more the nitrophenol concentration, the higher the adsorption competition with reductant (hydrogen from NaBH$_4$) and the reaction becomes significantly rate determining step than the absorbtion, hence, kinetic rate and conversion decreases.
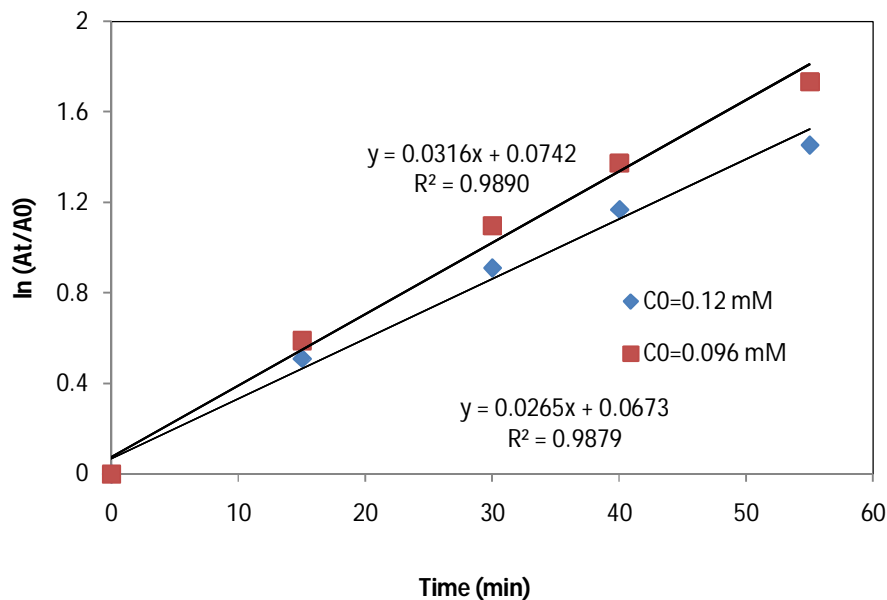
Figure 13. Plot of $\ln(A_t/A_0)$ versus time according to Eq. 3.4 for catalytic reduction of p-NP at two different initial concentrations with Palladium loaded flat sheet PES membrane in batch mode operation (Palladium loading = 0.318 mg, [NaBH$_4$] = 14.38 mM)

28

The rate constants were obtained from the slope of the kinetic curve at two different initial concentrations of p-NP, keeping other parameters such as shaking rate, borohydride concentration and Pa amount the same. An apparent reaction rate constant of 1.896 s^{-1} for 0.096 mM and 1.59 s^{-1} for 0.12 mM initial nitrophenol concentration was obtained in batch mode operation at the given experimental conditions; as depicted in Fig. 13. It was observed that with the increased initial concentrations the rate constant decreases. It was possible to see clearly the effect of time in batch mode operation as shown in Fig. 14.

a)   b)
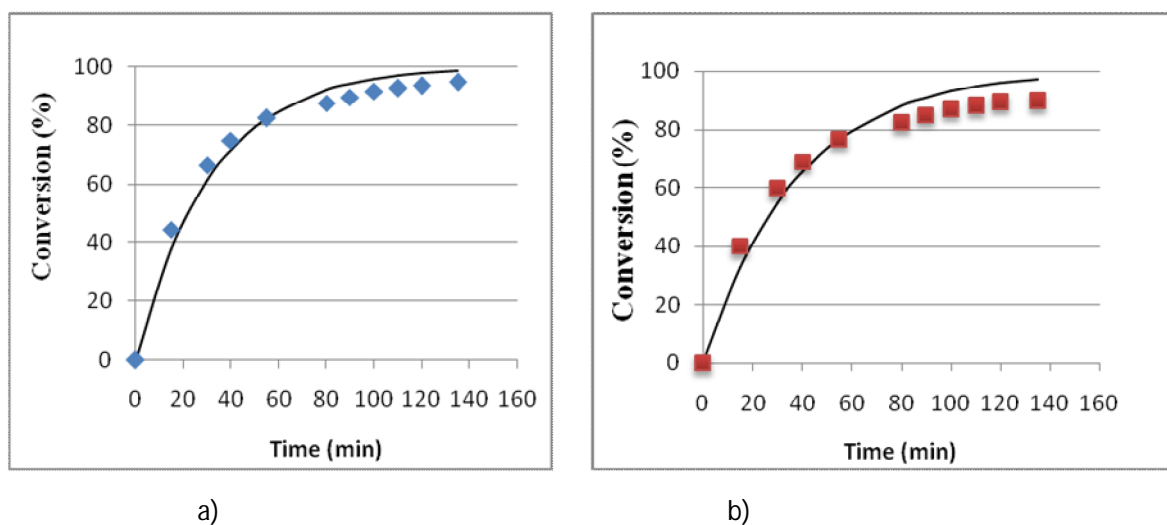
Figure 14. Exponential trend according to Eq. 3.6 ; for conversion versus time plot for p-NP reduction by NaBH$_4$ in Pd loaded PES membrane in batch mode. Conditions: a) [p-NP] = 0.096 mM, (b) [p-NP]= 0.12 mM, Pd = 0.318 mg; [NaBH$_4$] = 14.38 mM.)

As can be seen from Fig. 15, a batch mode reaction with lower concentration has higher conversion. This is related to the mechanism of catalytic reduction of nitrophenol using nanoparticles. As one of the surface reaction, the kinetics nitrophenol reduction using Pd is related to the active surface area on the catalyst. While keeping the active surface area constant, increasing the nitrophenol concentration will let majority of the reactant remained unreacted
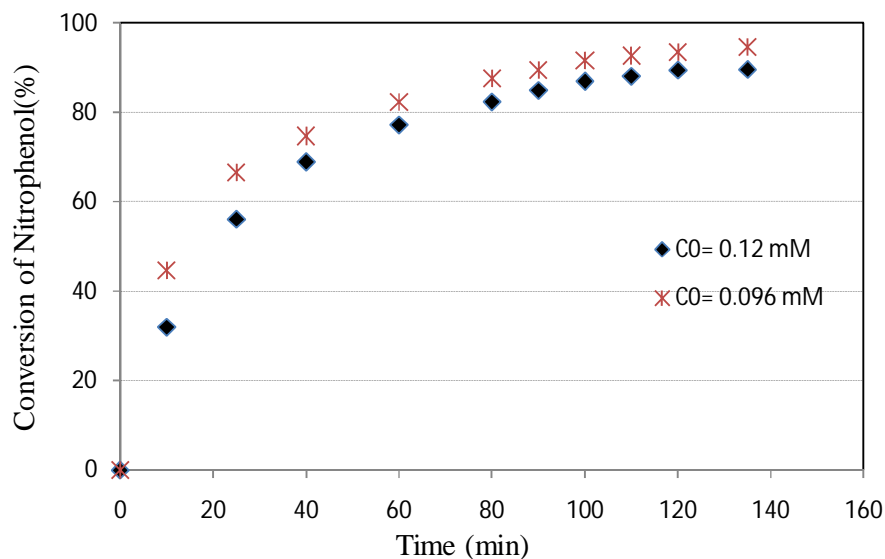
Figure 15. Conversion at two different Nitrophenol concentrations in two independent batch mode reactors, shaking at the same shaking rate with IKA shaker.

Normally, *p*-nitrophenol solution exhibits a strong absorption peak at 315 nm in neutral or acidic conditions, but upon the addition of $NaBH_4$ solution, the absorption peak shifts to 400 nm immediately, corresponding to color change (strong yellow) due to the formation of 4-nitrophenolate ion[49]. Fig 16. shows the UV-visible spectra of 4-nitrophenol reduction. As can be seen, the reduction reaction of nitrophenol in sodium borohydride does not proceed in the absence of catalyst. While filtering the solution in membrane supported Pd catalyst, the yellow color diminishes and the absorbtion becomes zero.
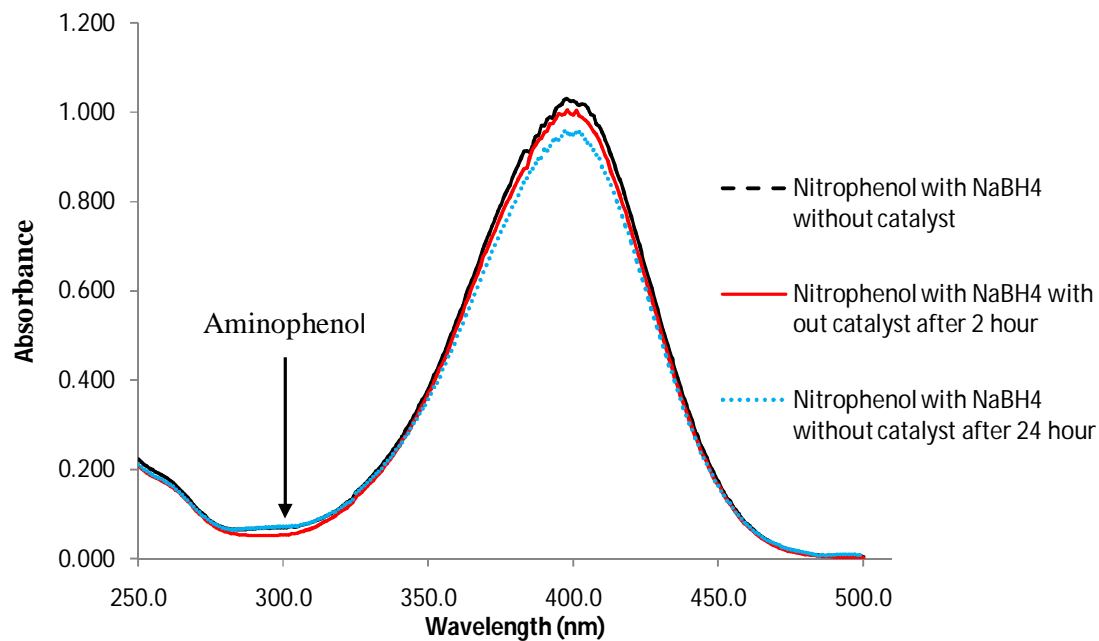
Figure 16. Absorbance spectra of aqueous solution of Nitrophenol and $NaBH_4$ in UV spectroscopy
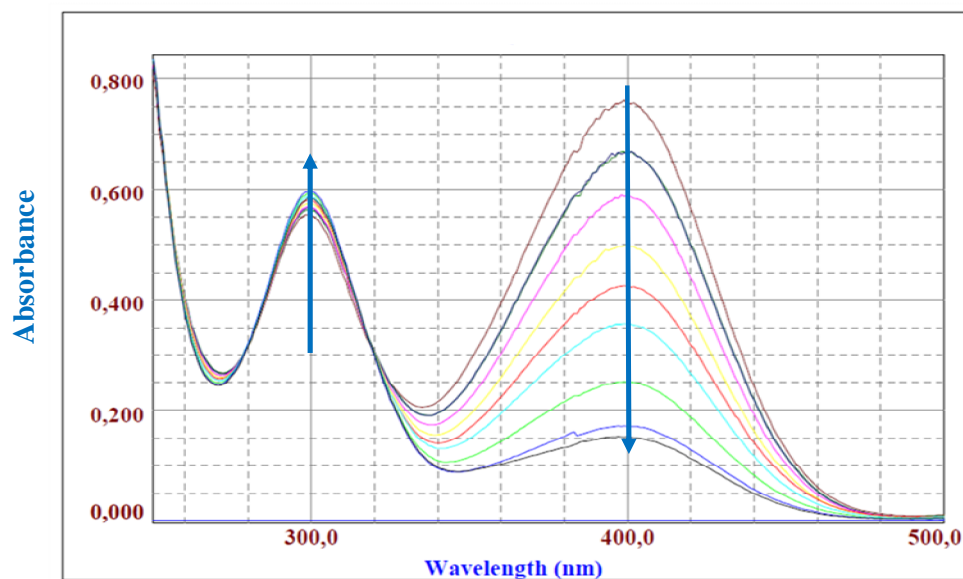
Figure 17. Absorption spectrum of p-NP reduction by sodium borohydride in Pd loaded PES membrane. The peak at 400 nm (nitrophenolate ions) is decreasing with reaction whereas a second peak at 300 nm (aminophenol) is slowly increasing.

Flow through reactor results

The experiments were carried out by forcing aqueous solutions of *p*-NP with different initial concentrations (0.033 - 0.514 mM) and sodium borohydride (14.38 mM) in the feed tank passing through palladium loaded membrane in a dead end filtration mode. In order to test the stability of the catalyst, three experiment at different initial nitrophenol concentrations (0.05, 0.08 0.144 mM), keeping all other conditions the same, were performed and the result is presented in Fig. 18. While keeping the feed pressure constant (flux) and catalyst weight the same, relatively constant nitrophenol conversion was achieved which is a strong indication that the nanoparticles showed stable reactivity at no disturbed conditions (no poisoning and deactivation). A long term stability was also checked after 24 and 48 h and the same conversion has been found, which affirms that the nanoparticles are strongly attached to the grafted layer and kept catalytically active.
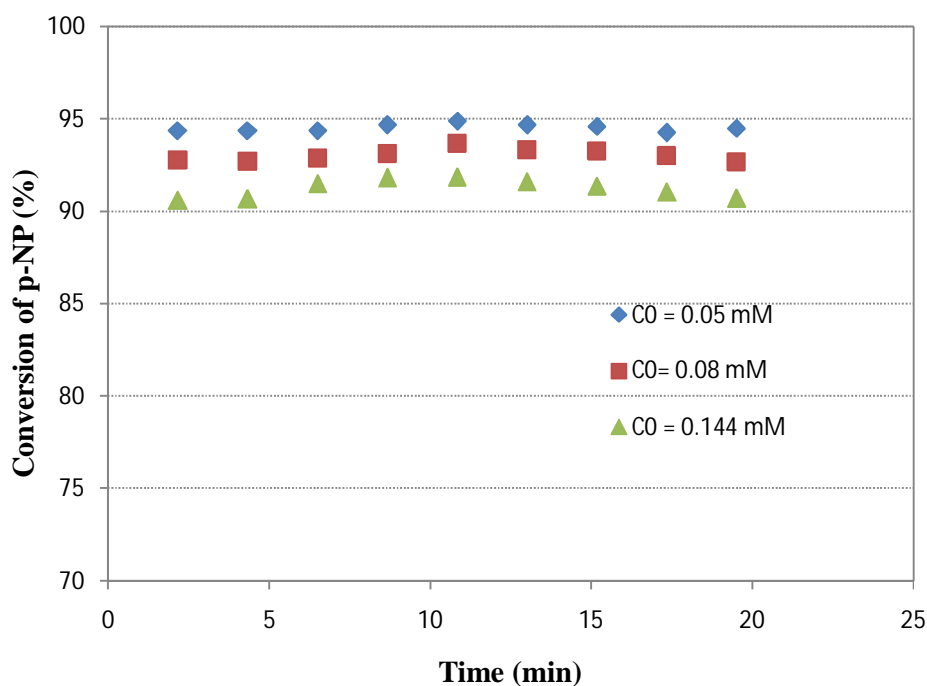
Figure 18. Effect of initial concentration on the conversion of NP at constant flux in single pass flow through membrane reactor, Conditions: palladium =. 0.282 mg, flux = 63 $Lh^{-1}m^{-2}$, [NaBH4] =14.38 mM)

Fig. 19 shows the effect of feed pressure; which is used to control the contact time; on conversion of nitrophenol. At lower feed pressure (i.e. at relatively higher contact time) , a complete conversion was achieved, whereas up on increasing feed pressure, hence shorter contact time between the Pd catalyst and reactant, the depletion of the reactants occurs at lower rate (lower conversion). In other words, a reaction at weaker and moderate convection regimes will result in no or negligible reactant concentration in the permeate side of the membrane ($C_A \approx 0$). The conversion profile result is in agreement with Lu Ouyang et al. [44, 50] used to test the nitrophenol reduction activity of gold nanoparticles in hollow fiber membranes prepared using layer-by-layer deposition of polyelectrolytes.
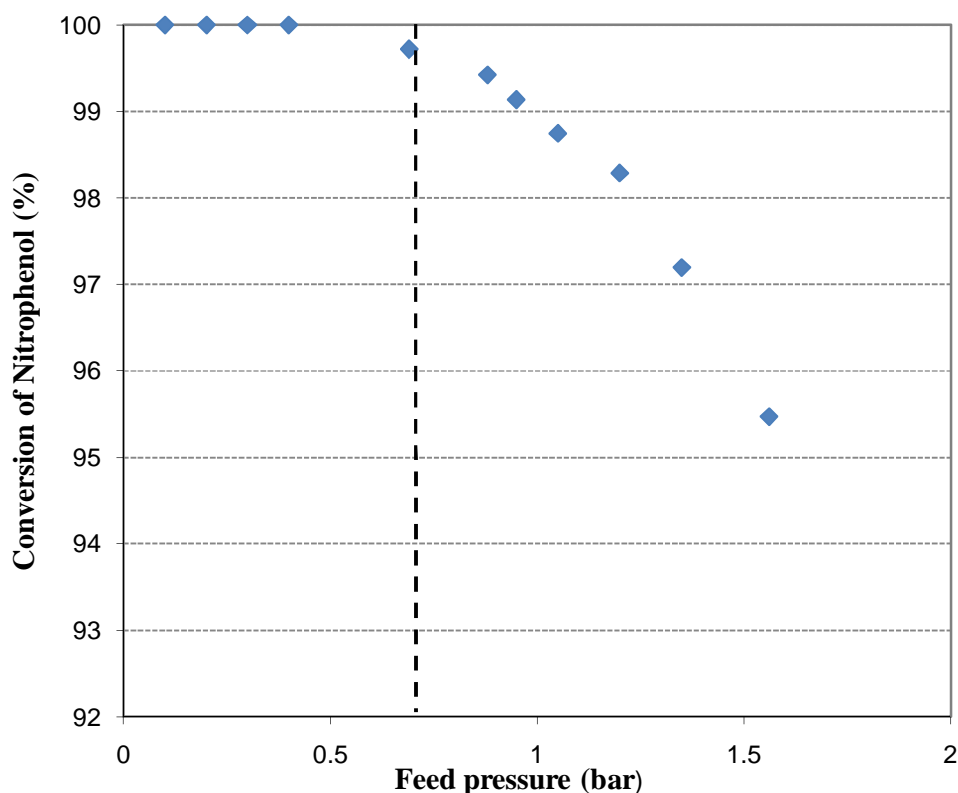
Figure 19. Effect of feed pressure on conversion of nitrophenol in single pass FTCMR at conditions of ([p-NP] = 0.514 mM, [NaBH$_4$] =14.38 mM, and Pd amount = 0.733mg)

From this experiment, we can define an effective contact pressure, the pressure regime at which complete conversion is achieved or the pressure regime in which no nitrophenol concentration escapes the FTCMR. For example this contacting pressure will be an important parameter in applications where complete destruction of nitrophenol is mandatory or to meet

the minimum   legislative *p*-NP concentration requirements in effluents. The available catalysts are only capable of complete conversion in certain concentration limits with single pass operation, as the reaction is becoming significantly limited by the surface reaction.

The transmembrane pressure was continuously changing so as to control and vary the permeate flux. The conversion of *p*-NP in the permeate is plotted as a function of permeate flux; as shown in Fig. 20. As can be seen, conversion was found to be decreasing with increasing flux. This is related to the contact time of the reactant and catalyst. Increasing transmembrane pressure reduces the hydrodynamic residence time of *p*-NP in the grafted catalytic layers, which leads to insufficient contact time to achieve higher (complete) conversion. Additionally the reaction rate is limited by a low number of available catalytically active sites due to the surface coverage, hence decreasing conversion as a function of the flux was observed. The same results were reported by Clélia Emin et al. [10] and Westermann et al. [25]

The effect of the nitrophenol concentration in the feed on its conversion was also investigated using different feed concentrations and the same amount of Pd at a room temperature. A closer look at on Fig. 20, clearly shows the effect of initial   *p*-NP concentration on conversion. As the same result obtained for batch mode, the conversion is higher for the lower *p*-NP initial concentration. In all of our initial *p*-NP concentration ranges (i.e. 0.033-0.514 mM), the same trend was obtained, which strongly indicates that this reaction on Pd nanoparticle is highly active surface dependant. For the same catalyst loading and permeate flux (i.e., approximately the same residence time and applied pressure within a membrane), the catalytic activity of membranes with lower initial concentration was higher than that of higher initial NP concentration.

Furthermore, the inverse proportionality of *p*-NP conversion with permeate flux confirmed that our Pd loaded membranes were not mass transfer limited; rather it was reaction limited. If membranes were mass transfer limited, we would not be observed a decrease of conversion with increased fluxes. As the applied pressure in flow through mode enforces reactants to have an intensive contact with catalyst, the reaction at the surface of the catalyst is the main limitation to such system. As a result of increasing pressure (flux), reactants permeates through the membrane without reacting, hence the conversion decreases. Similar results were reported by David M. Dotzauer et al. [51] and Christopher et al.[52]
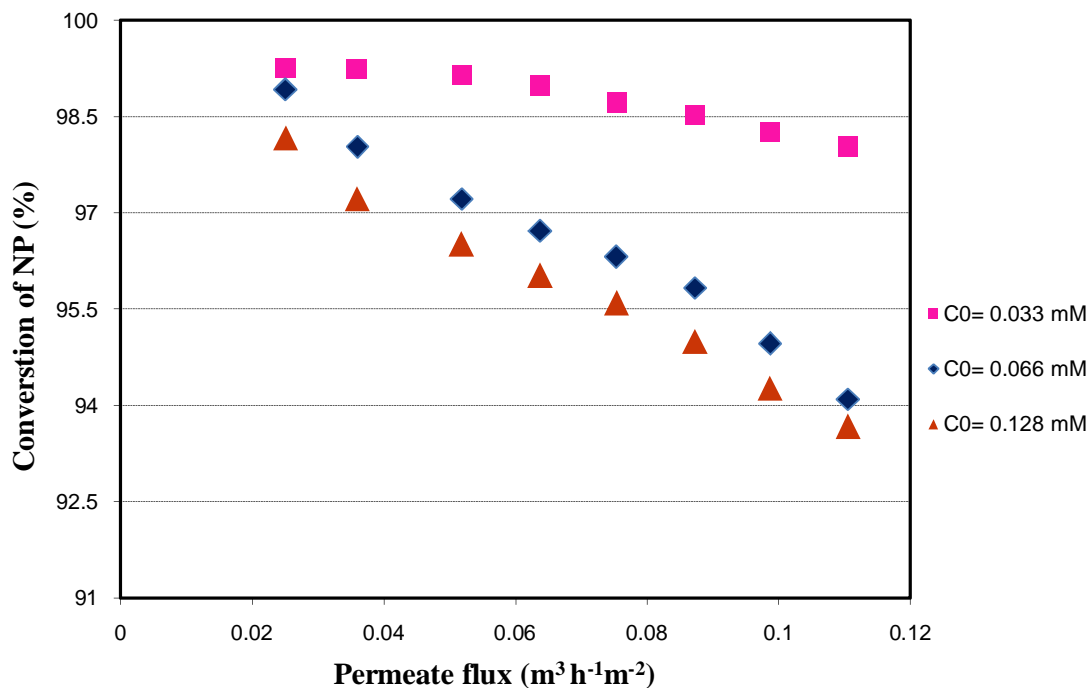
Figure 20. Conversion of Nitrophenol (NP) in Pd loaded PES membrane versus flux for single pass in dead end mode of filtration at different initial concentrations of nitrophenol (Palladium amount = 0.283 mg)

With increasing fluxes, conversion was declined as it was expected. Still, as Figure 20 shows, conversion is greater than 93% at fluxes below 120 LMH (0.12 $m^3 h^{-1} m^{-2}$). The maximum pressure used to fix the flux in our system was limited to about 1.8 bar; as higher applied pressures can result in membrane fracture.

The effect of convective flow on nitrophenol conversion has also been investigated in different initial concentration ranges and the results are presented in both Fig. 21 and 22. The experiments clearly revealed that for the FTCMR, depending on the initial concentration of p-NP and the amount of catalyst used, there are an effective convective pressure during which no p-NP escapes the reactor.
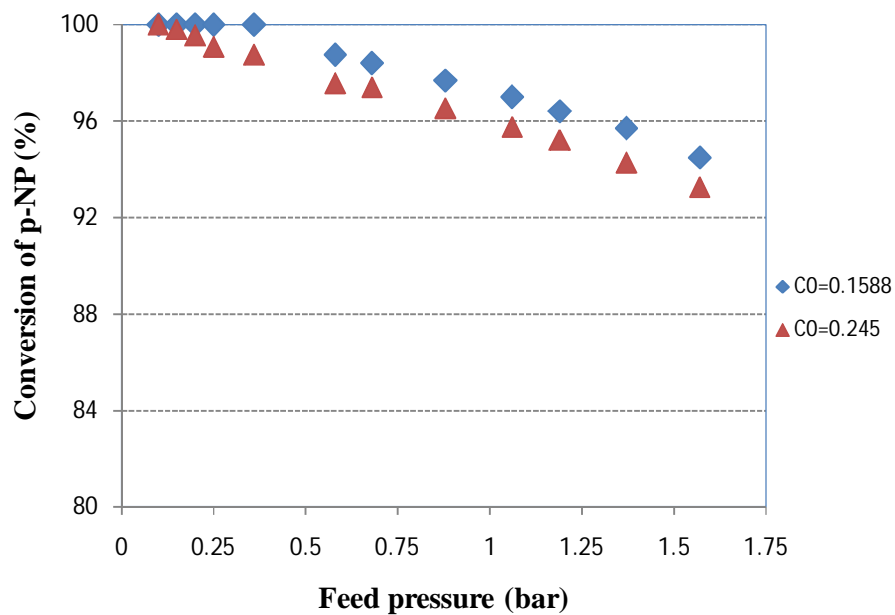
Figure 21. Effect of Initial p-NP concentration on conversion as a function of feed pressure (palladium = 0.715 mg)
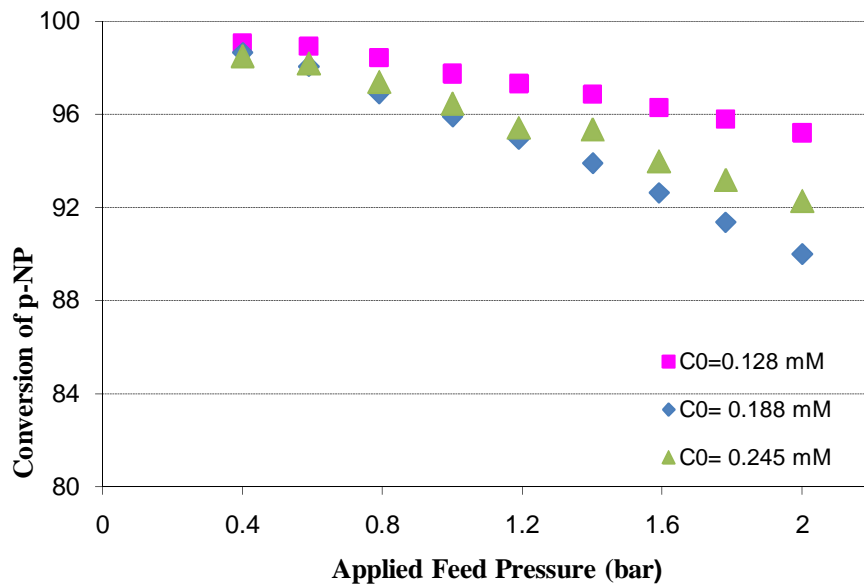
Figure 22 Figure 21. Effect of Initial p-NP concentration on conversion as a function of feed pressure (palladium = 0.715 mg)

The data in Figure 23 shows, the experimental points and fitted according to Eq. (3.3) and it conforms well to a simple first-order kinetic model of the reaction.
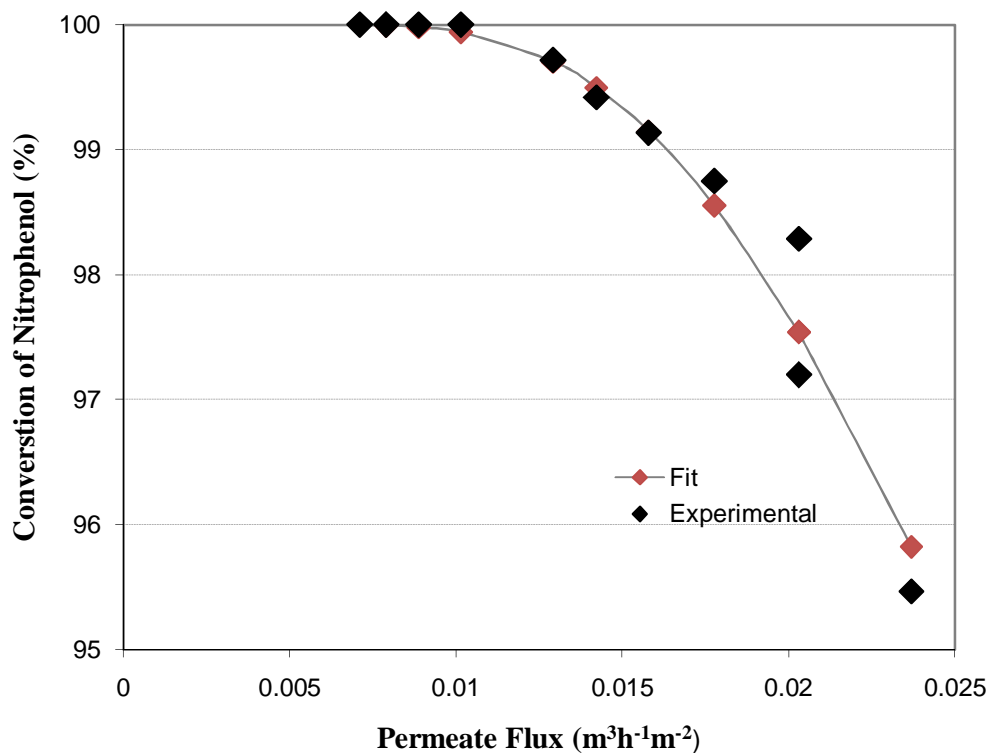
Figure 23. Plot of *p*-NP conversion versus flux for membrane containing Pd. The curve(with red diamond) represents a first-order reaction model according to Eq. (2.3) with a rate constant (*k*) of 0.114 $s^{-1}g^{-1}$. Feed conditions: [*p*-nitrophenol] = 0.514 mM, [NaBH4] = 14.38 mM, Pd = 0.733 mg

The effect of catalyst weight was also evaluated by taking five different membranes grafted at different energies. The experiments were carried out at constant flux of 60 LMH in order to test only the catalyst weight in flow through reactor mode. The results are shown in Fig.24. As increasing the amount of catalyst increases the catalyst surface area, the increase of conversion was expected according to Eq. 3.5.
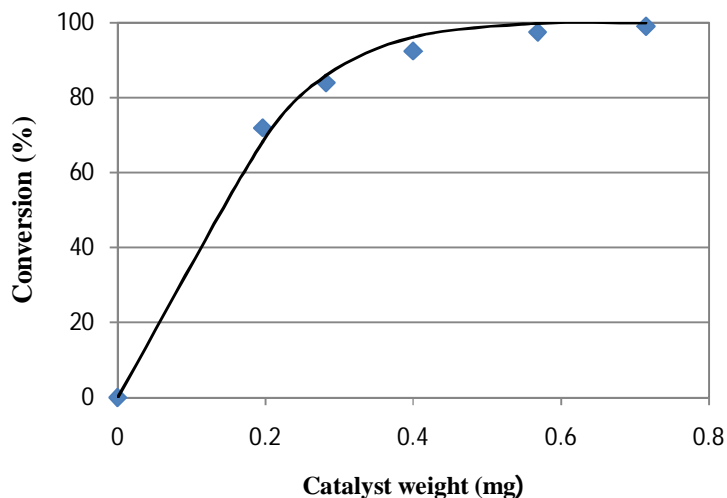
Figure 24. Effect of catalyst weight on conversion. The blue diamond are experimental points and the curves represent the fit values according to Eq. 3.5 Conditions: [p-NP] = 0.128 mM, [NaBH$_4$] =14.38 mM
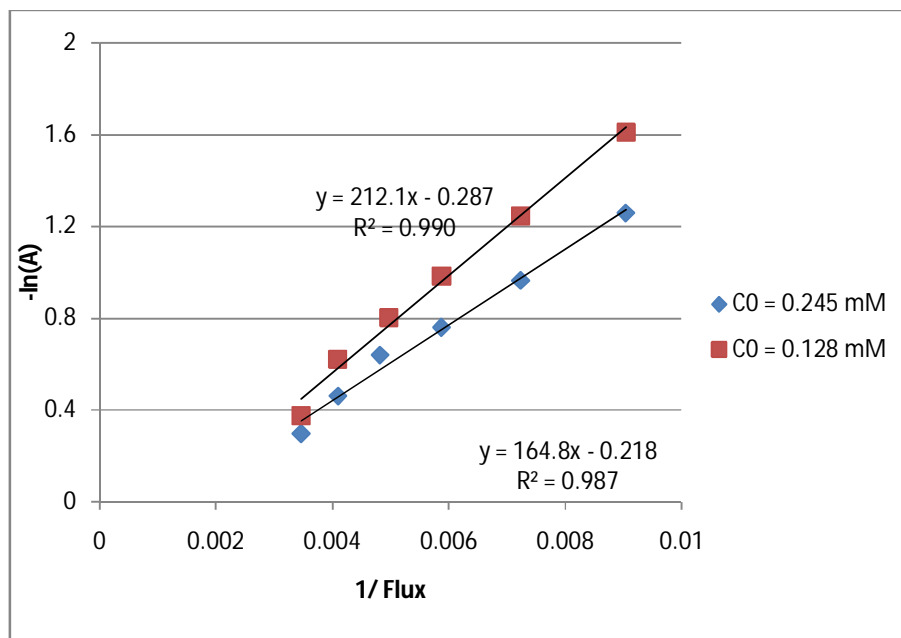
Figure 25 Plot of ln (A) versus 1/ Flux , the slope is Kpp (apparent kinetic constant) based on Eq. 3.3, Conditions: Pd amount = 0.715 mg, [NaBH4] = 14.38 mM

The effects of nitrophenol concentrations on the apparent rate constant in flow through reactor mode is shown in Fug. 25. As it is shown in the figure, at 0.128 and 0.245 mM initial nitrophenol concentrations, rate constants of 212.1 h^{-1} (0.0824 s^{-1}g^{-1}) and

164.8 h^{-1} (0.064 s^{-1} g^{-1}) were found respectively. This result shows the same trend with our batch mode of operation, in a way that the rate constant is lower when the initial concentrations are increasing. The same results were reported by Stefanie et al.[46]

Simulation Results

In order to understand better and check the effect of different parameters, numerical simulations of the FTCMR were performed using Wolfram Mathematica 7, at different process parameters such as peclet number, reaction modulus, catalytic membrane layer thickness and concentrations; using Eq. 3.1- 3.3. According to our simulation results, majority of our experimental results seems following the same profile.
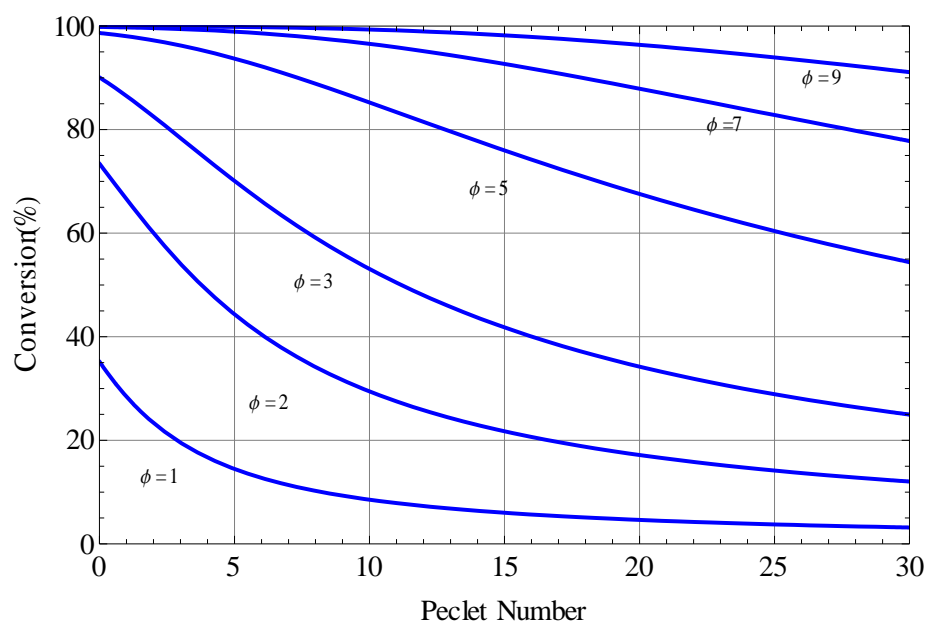
Figure 26. Conversion versus convective flow (peclet number) at different values of reaction modulus based on Eq. 3.2
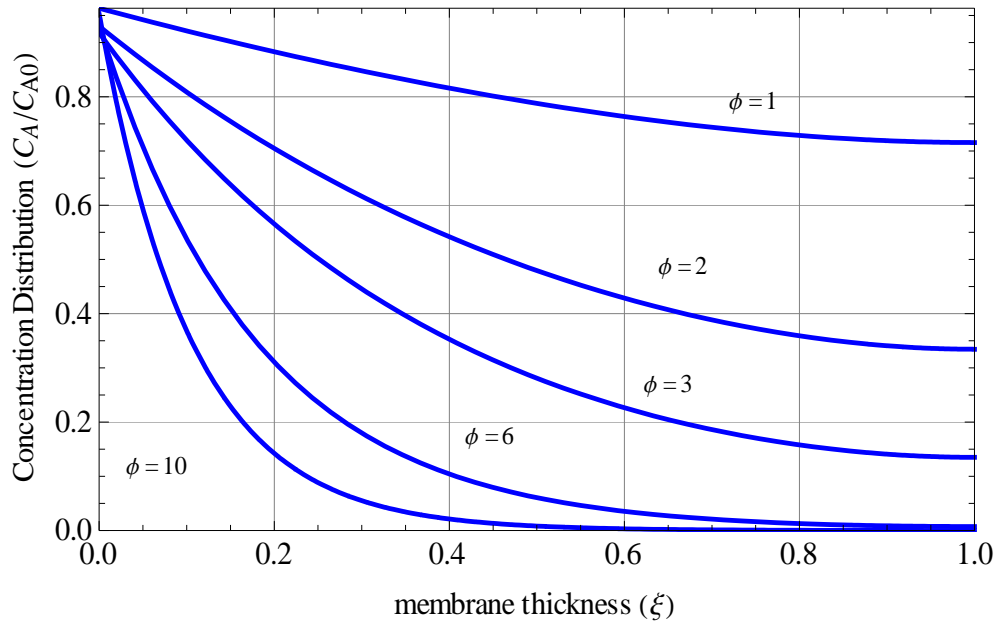
Figure 27. Concentration distribution across the catalytic layer at different values of reaction modulus, according to Eq. 3.1
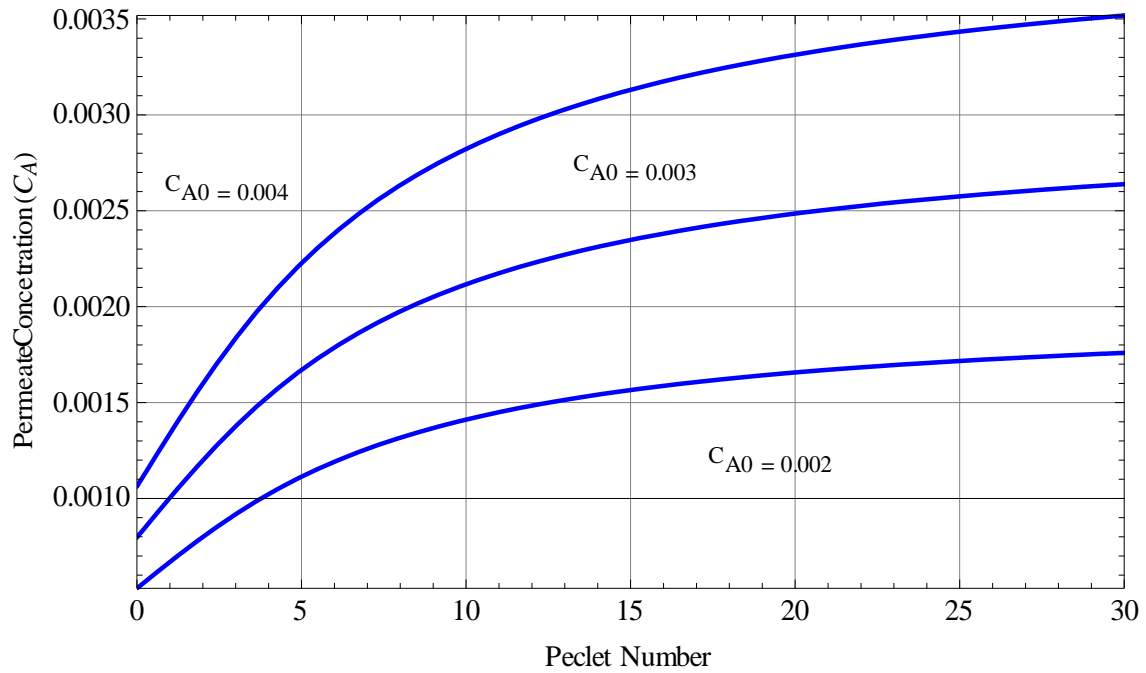
Figure 28. Reactant concentration profile at the exit of the catalytic layer (permeate side concentration) with different initial concentrations and reaction modulus of 2. based on Eq. 2.
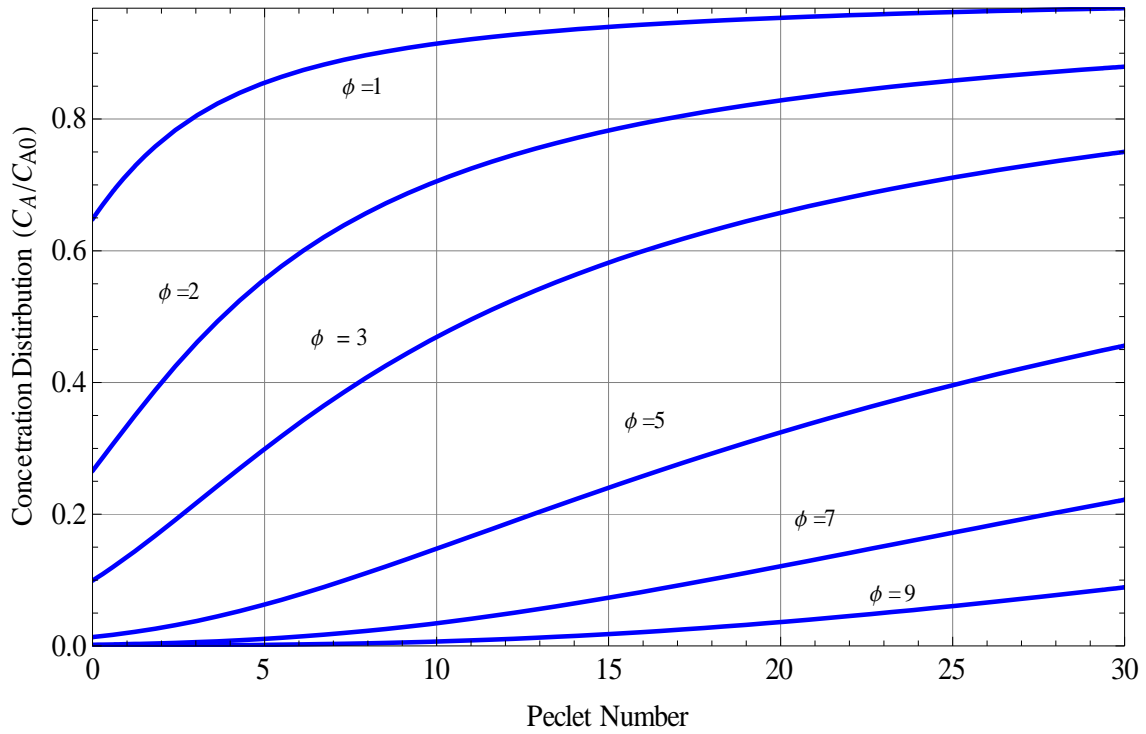
Figure 29 Concentration distribution versus peclet number at different reaction modulus, based on Eq. 3.2
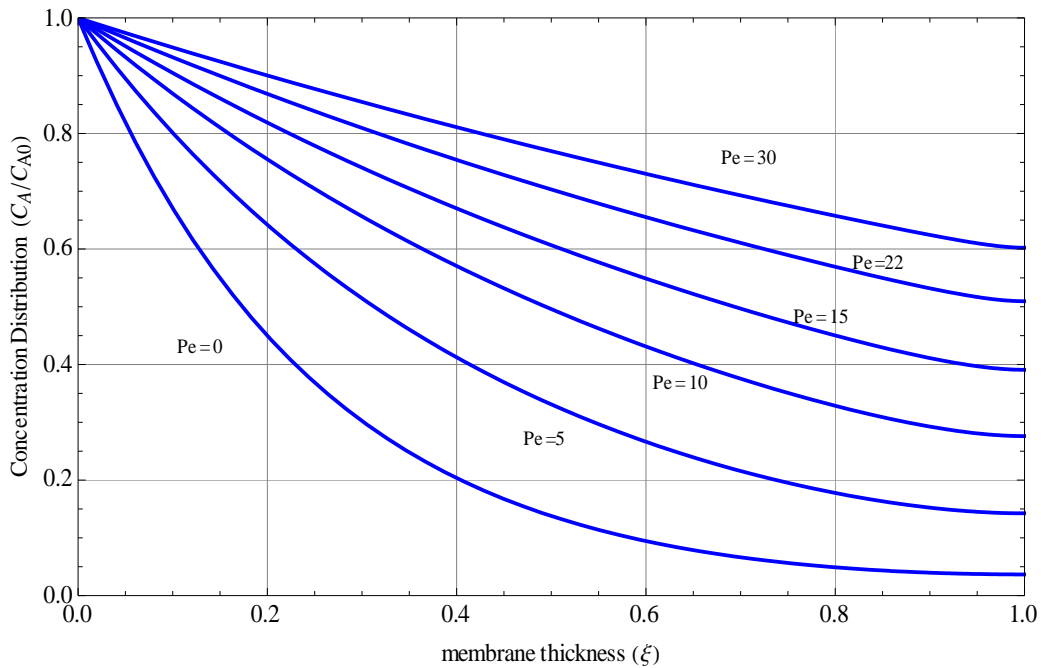
Figure 30 Concentration distribution versus membrane thickness at different values of peclet number, based on Eq. 3.1
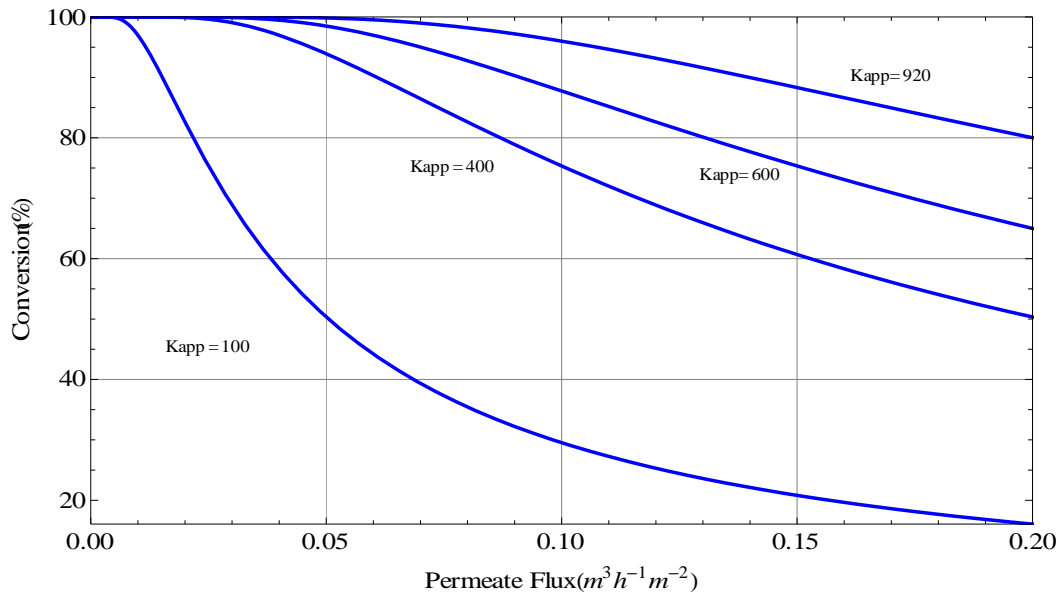
Figure 31 Conversion versus permeate flux at different values of apparent kinetic constant in (h^{-1}) based on Eq. 3.3

4. Catalytic polymer membranes for Gas/Liquid contacting

4.1 Introduction

Gas/liquid reactions are widely applied in multitude range of processing sectors; such as chemical, petrochemical, food processing, biotechnological and environmental industries. Catalysts are very often used in these processing industries aimed at decreasing the required reaction temperature and minimizing the formation of unwanted side products and intermediates. Although homogeneous catalysts can be sometimes more active and selective to the desired products, heterogenous catalysis has a preferential advantage by the industry because of its easy catalyst separation from the whole reaction mixture. However, the use of solid catalysts in gas/liquid reaction incurs a challenge to reactor design, as it leads to multiphase phase (gas/solid/liquid) system[39].

For gas/liquid reactions, an intensive contact between two phases can be achieve by; dispersing gas bubbles into bulk liquid, creating liquid droplets in the gas and establishing a thin liquid film having interfacial contact with the gas [50]. Different conventional contactors such as; falling-film columns, packed columns, bubble column, spray tower, gas-liquid agitated vessel, and plate columns; are used to provide an interfacial contact area for the two phases. However, in majority of these contactors the reaction is mainly limited by gas

solubility in the bulk liquid as a result usually higher pressure is applied in order to increase its solubility.

In recent times, membrane contactors become promising alternative for gas/liquid reactions to overcome drawbacks of traditional contactors. Membrane contactors are advantageous over conventional gas/liquid contactors in providing large interfacial surface area per unit volume, compact and modular design, relatively easy for scale up, high operational stability and flexibility and lower energy consumption[53]. Membrane contactors are usually applied in shell-and-tube configuration containing microporous capillary hollow fiber membranes; with sufficiently small pores so that capillary forces prevent direct mixing of the phases on either side of the membrane. The role of the membrane is to provide interfacial contact area for gas and liquid phases, but does not perform selective separation. For stable operation and high mass transfer coefficient, the membrane material must be non-wettable for the liquid phase; to make ensure the pores are free of liquid. However, when the membrane pores are filled with the liquid (wetted), the membrane mass transfer resistance becomes significant and will not be economically viable. Hence, long-term stable operation of membrane contactor requires, gas filled pores (non-wetted condition) over longer operational time. The wetting tendency of a gas/membrane/liquid combination is mainly determined by membrane properties; such as pore size, liquid properties such as surface tension, and their combined interactions. Liquids having lower surface tensions tend to wet the surface more easily than liquids with higher surface tensions[50].

The gas–liquid membrane contactors are often catalytically active; where catalytically active layer faces the liquid side and the gas phase diffuses through it and dissolves in the liquid at the interface. Therefore, membrane contactors offer unique features of nondispersive gas-liquid contacting and introduction of reactants at different sides of a membrane allows independent control of the flow rate of reacting streams. The gas pressure can be varied between the wetting pressures of the support layer and that of the active layer. As a result of pressure gradient, the reaction products preferentially diffuses in the direction of liquid side. One important feature of membrane contactor is that, high pressures are not required; even for low solubilities, as the gas is supplied directly where it is consumed.

Flow through membrane reactor experiments are found in literature applied for varies hydrogenation reactions. The selective hydrogenation of propyne to propene has been studied

over porous ultrafiltration polymeric membranes of polyacrylonitrile (PAN), polyetherimide (PEI) and polyamideimide (PAI) over poly acrylic acid membranes treated with palladium acetate [11]. Similarly, porous PVDF membranes loaded with palladium nanoparticles were used for hydrogenation of methylenecyclohexane by flow through experimental setups[54]. Besides, the hydrogenation of viscous liquids such as vegetable oils have also been performed in flow through experiments over porous polymeric membranes loaded with palladium and platinum nanoparticles [55].
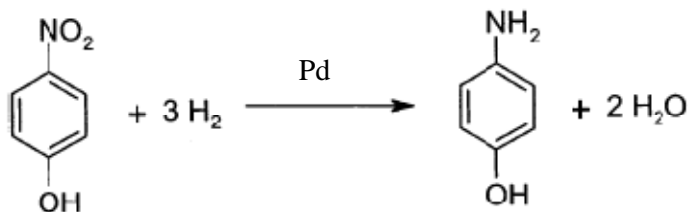
Figure 32. Schematic diagram of catalytic hydrogenation of p-nitrophenol to p-aminophenol[56]

p-Aminophenol is industrially an important intermediate fine chemical in the preparations of analgesic and antipyretic drugs. It is also used as a developer in chemical and dye industries. Various synthesis methods have been reported in literature to prepare *p*-aminophenol, such as iron-cid reduction of *p*-nitrochlorobenzene or *p*-nitrophenol, and catalytic hydrogenation of nitrobenzene [57]. The major disadvantage of the iron-acid reduction method is the generation of large amounts of Fe-FeO sludge, which cannot be reused and causes severe disposal problems. The catalytic hydrogenation of nitrobenzene in a strong acid aqueous medium is an important commercial method, but it has two main drawbacks, i.e. the formation of side products such as aniline; and the use of highly corrosive mineral acid. Therefore, synthesis of *p*-aminophenol using direct catalytic hydrogenation of *p*-nitrophenol is an efficient and greener synthesis route[58].

The production of such fine and speciality chemicals, and intermediates requires highly selective chemical processes with nearly complete conversions in mild reaction conditions. Recently, Rahat Javaid et al.[59] have carried out hydrogenation of *p*-nitrophenol in the presence of formic acid by passing the reaction solution through the catalytic tubular reactors, where, the inner surface of a metallic tube was loaded with Pd nanoparticles. *p*-Aminophenol was produced as a sole product of hydrogenation without any side reaction. Rizhi Chen et al.[60] has successfully developed a membrane reactor by depositing palladium nanoparticles

on a hollow fiber ceramic membrane support in which the support surface was silanized with aminofunctional silane. The catalytic property was evaluated by the hydrogenation of *p*-nitrophenol to *p*-aminophenol as a model reaction and compared with the catalytic property of palladium nanoparticles deposited on a tubular ceramic membrane support. The catalytic activity of Pd-loaded hollow fiber ceramic membrane support was significantly higher than that of Pd-loaded tubular ceramic membrane support. This is due to the fact that, the hollow fiber ceramic membrane can provide more membrane area for the deposition of palladium nanoparticles at the same volume of membrane module than tubular ceramic support.

In this research, surface modified commercial hollow fiber PES microfiltration membrane via photochemical graft polymerization of AA and embedded with palladium nanoparticles with nearly dense property is tested to synthesize *p*-aminophenol via direct hydrogenation of *p*-nitrophenol; as a model for gas/liquid contacting. In a very recent publication of Clélia Emin and coworkers[10], the effect of UV irradiation energy and monomer concentration on the permeability of the membrane has been evaluated. The more the energy received by the membrane during photografting, the lower permeable it becomes. It is clearly shown in the following figure that, the modification of the membrane is done by compromising its permeability, which seems non sensible from the perspective of improving the economic viability of membranes by enhancing their permeability. From the other way round, this kind of membranes could be very important for gas/liquid contacting as a dense membrane. Based on this premises, all experiments were carried out at the same experimental conditions indicated below in the figure so as to modify the membrane in a way that can be applied for gas/liquid contacting.

45
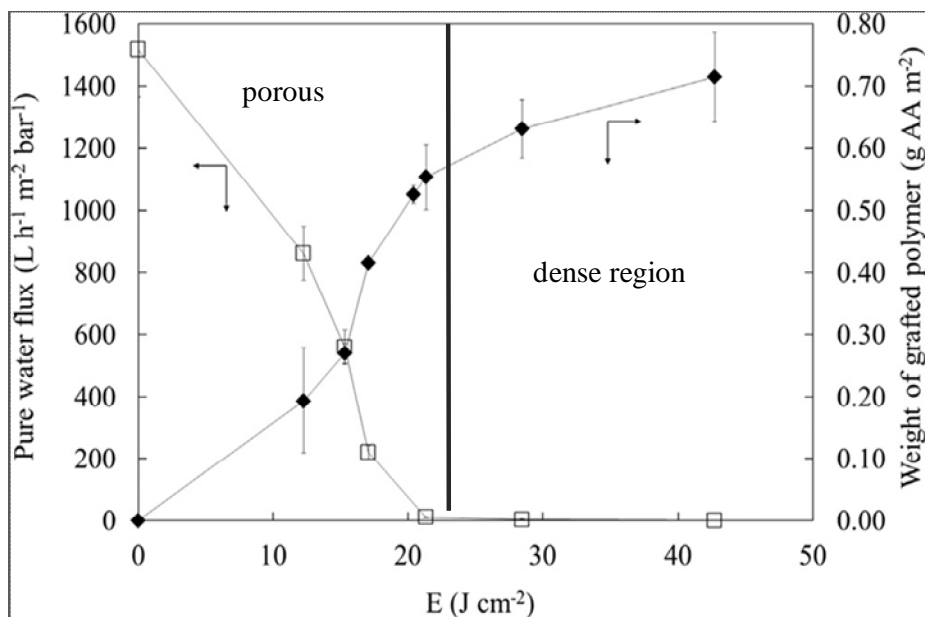
Figure 33. Effect of UV irradiation energy on pure water permeability of modified membrane
Experimental conditions: [AA] =25 wt%, [Photoinitiator] = 0.03 mol%, [cross-linker] = 2.7
mol%.[10]

4.2 Experimental

4.2.1 Materials and Methods

Materials

The following chemicals and materials were used during the experiment. acrylic acid, N,N'-methylene-bis-acrylamide, 4-hydroxybenzophenone, sodium borohydride, tetra-ammine palladium(II)chloride monohydrate, and p-nitrophenol (*p*-NP) from Sigma Aldrich France, PES Micro PES® from Membrana (Wuppertal, Germany) which has a nominal pore size of 0.2 μm, an inner diameter and thickness of 300 and 100 μm respectively. All compounds have been used without any purification and solutions were prepared with deionized water.

Photografting Experimental Setup

UV induced membrane surface modification was performed on commercial hollow fibre MF PES membrane using a continuous photografting reactor. The photografting setup is shown below in Fig.30 Initially, the hollow fibre membrane was passing through a solution

containing; acrylic acid monomer (25 wt. %), water (72 wt.%), a photo initiator of 4-hydroxybenzophenone (0.1 mol %) and N,N`-methylene-bis-acrylamide (5 mol%) as cross-linker. The photo initiator (sensitizer); up on UV irradiation decomposes into reactive free radicals which initiate monomer graft polymerization on membrane surface, while the role of the cross linker is to form polymer networks during polymerization. The rotating speed of bobbin in the photo reactor setup was adjusted to 8 m/min and a relatively higher energy per membrane area (about 22 J/cm^2) was applied to proceed at complete photografting polymerization, so that dense layer can be grafted over the outer surface of the hollow fiber. Then, the membrane was passed through two independent industrial UV polychromatic lamps (UVAPRINTLE, doped halogen lamps, I= 5520–10080 mWcm^{-2}, Hoenle UV France, Lyons, France). In the first lamp, free radicals are formed and photografting starts, while in the second lamp, further polymerization and cross linking took place. After grafting, the membranes were washed with deionized water in order to remove any excess monomer and a homopolymer which is not strongly attached to the membrane. The presence of any un reacted monomer paves the way for aggregation of nanoparticles. Then pure water permeability was tested using lab made module in cross flow filtration mode. A dried sample was taken for surface analysis using attenuated total reflection fourier transform infrared spectroscopy (ATR-FTIR, Thermo-Nicolet Nexus).
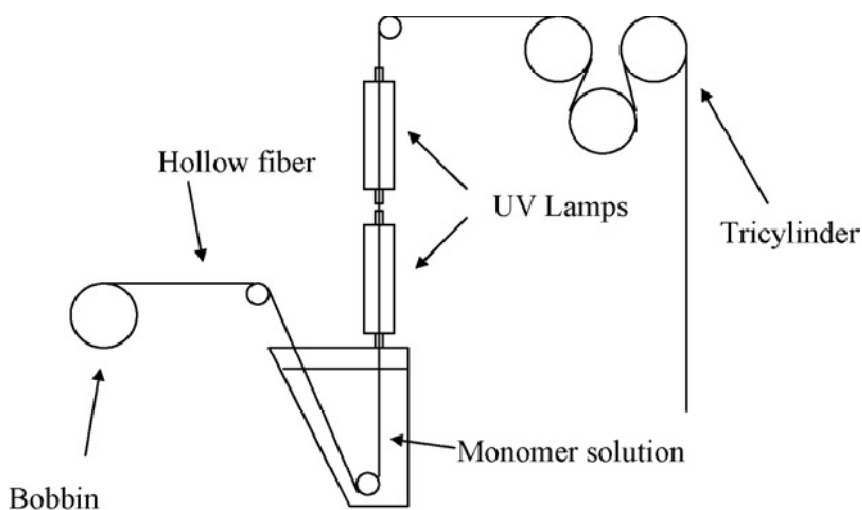
Figure 34. Continuous Photografting reactor setup

Palladium nanoparticle synthesis

The synthesis of Pd-NPs inside functionalized hollow fiber PES membrane was carried out via Intermatrix synthesis method with the following procedures[6, 7]: (1) Functionalized hollow fibbers were dipped in to palladium salt $[Pd(NH_3)_4Cl_2.H_2O]$ 0.01M solution, which leads to ion exchange reaction between Pd^{+2} and carboxylic groups on surface of functionalized hollow fiber membrane (Eq.1). The cation exchange was performed over night at room temperature and (2) metal ions loaded on hollow fibers reduced with 0.1M aqueous solution of $NaBH_4$ (Eq. 2). Finally, the fibers were rinsed and washed with pure water in order to remove excess un reacted substrates. Up on reduction using $NaBH_4$, the white hollow fiber becomes grey in color.

$$2R–COO^-H^+ + [Pd(NH_3)_4]^{2+} \rightarrow (R\text{-}COO^-)_2[Pd(NH_3)_4]^{2+} + 2H^+ \text{---------------(1)}$$

$$(R\text{-}COO^-)_2[Pd(NH_3)_4]^{+2} + 2NaBH_4 + 6H_2O \rightarrow Pd^0 + 7H_2 + 2(R\text{-}COO^-)Na + 2B(OH)_3 + 4NH_3$$

$$\text{------------(2)}$$
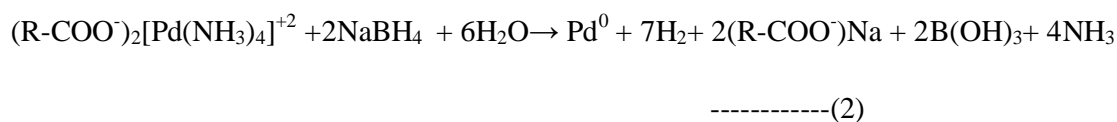
Hydrogenation Pilot Experimental Setup

The hydrogenation experimental setup is shown in Fig.24. The module containing Pd embedded hollow fiber membranes is prepared and installed to the hydrogenation pilot equipment. The molecular hydrogen gas and aqueous p-NP solution at different initial concentrations (0.033- 0.345 mM) were flowing in countercurrent flow configuration in the module containing the catalytic membrane, where the catalyst is placed exclusively in a thin grafted surface layer of hollow fiber for running gas/liquid reactions. In this mode, liquid nitrophenol solution is pumped from the feed tank to flow through the shell side of the module, while hydrogen gas flows in the lumen side of the hollow fibers. The flow rate of hydrogen is controlled by adjusting the feed pressure ranges (1 - 7 bars).
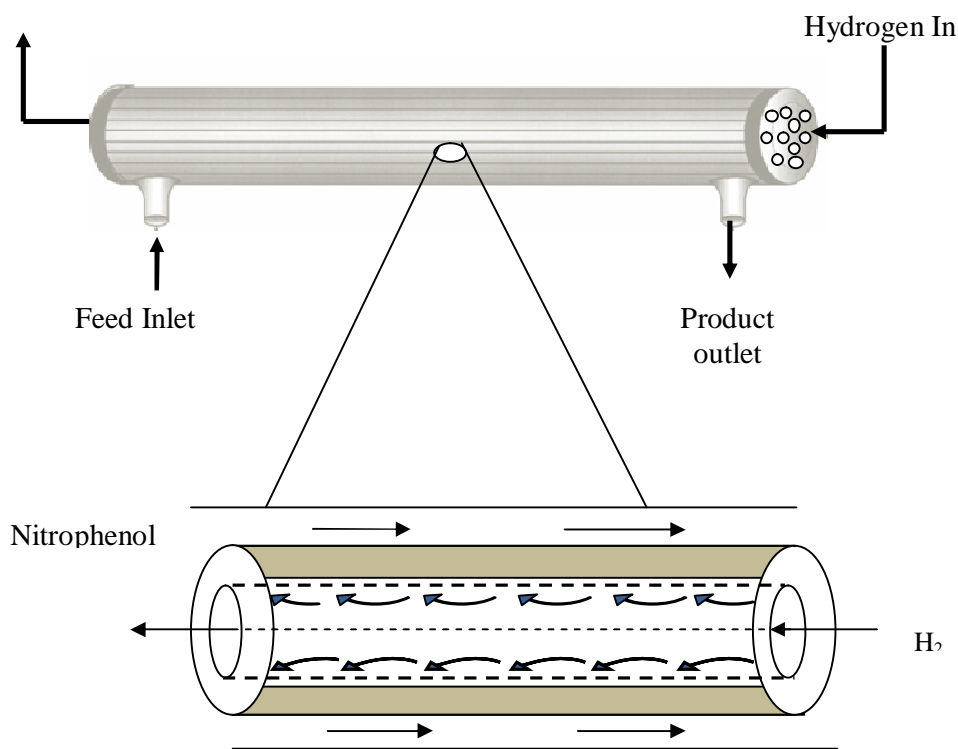
Figure 35. Schematic flow diagram for the hydrogenation of *p*-NP in a catalytic polymeric hollow-fiber reactor, countercurrent flow configuration of module and hollow fiber.

4.2.2 Results and discussion
ATR-FTIR Results

The ATR-FTIR spectra of unmodified and modified commercial hollow fiber PES membrane with AA (25 wt %) are shown in Fig. 33. Acrylic monomers possess a hydroxyl (O–H) functional group which can be determined in the IR spectrum at 3400–3600 cm^{-1}; whereas, carbonyl group (C=O) is usually located at 1620–1750 cm^{-1}. In the spectrum; in addition to the typical PES absorption bands of the unmodified membrane, the IR spectra of modified membrane has a new absorbtion peak at 1730 cm^{-1}, which corresponds to the stretching

vibration of carbonyl (C=O) groups [1]. It can be clearly seen that the acrylic monomers were grafted onto the PES membrane surface. In the spectra of AA-modified membranes, there exists bands of vibration at 3460 cm^{-1}. These bands can be attributed to the hydroxyl groups present in the photochemically modified membranes. This is not visible for the unmodified membrane [61].
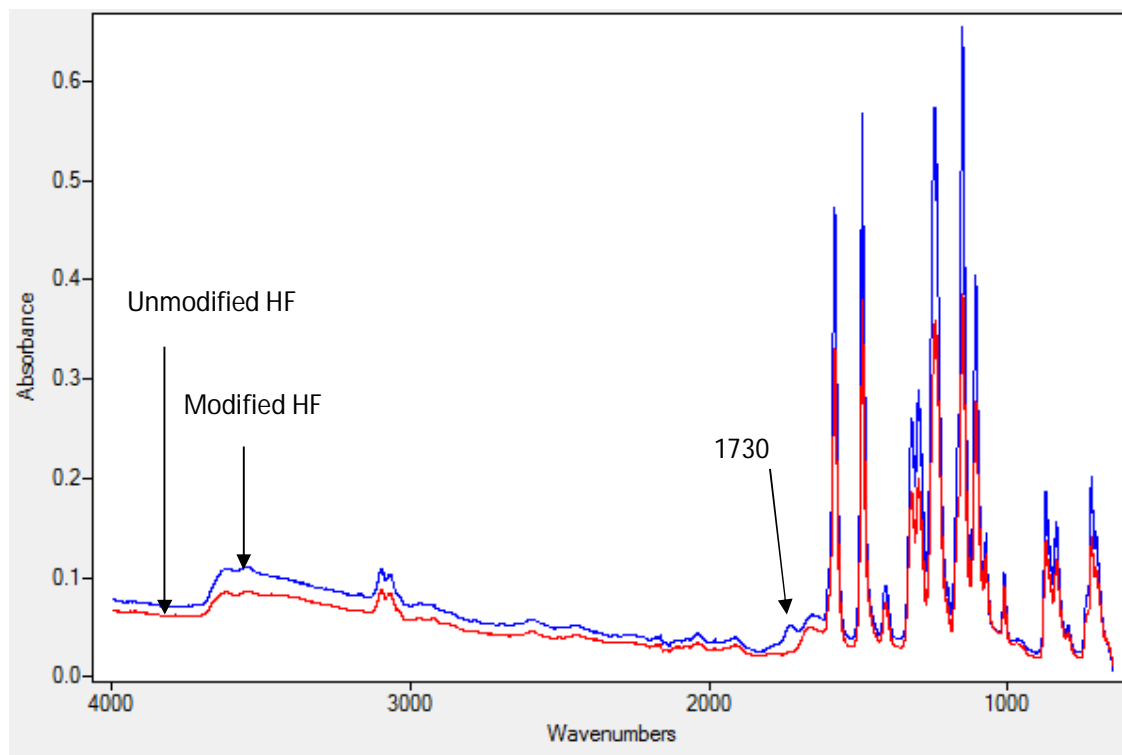
Figure 36. The ATR-FTIR spectra of the unmodified Hollow Fiber (HF) PES membrane and the modified membranes with 25 (wt %) acrylic acid at UV-irradiation time.......

Hydrogenation Results

The reaction of p-nitrophenol reduction with molecular hydrogen was performed in Pd loaded membrane, which was chosen as a model reaction for gas/liquid contacting. At the given grafting experimental conditions, it was possible to successfully modify the membrane with nearly a dense permeability which can be applied for gas/liquid contacting. However, under our experimental conditions the reaction was failed to undergo hydrogenation with our Pd loaded membrane and no reaction progress has been observed with the spectroscopy.

Hydrogenation of aqueous *p*-nitrophenol (0.033 - 0.345 mM) was carried out with hydrogen pressures, (1-7 bars), and feed temperatures in the range of (298–313 K) using Pd loaded membrane as catalysts in a relatively dense membrane contactor. Hydrogenation of *p*-nitrophenol under all the above conditions was not successful to produce the desired product , i.e. p-aminophenol. Hydrogen failed to reduce p-nitrophenol at all in all experimental conditions using Pd embedded PES membrane contactor.

From our experimental result in liquid phase hydrogenation of nitrophenol using borohydride, we observed that this reduction reaction is highly dependent on initial concentration of nitrophenol. An increases in *p*-NP concentration incurs a surface adsorption competition with hydrogen from borohydride and result in decrease of conversion. Taking in to account of this, hydrogenation was also carried out in a 'catalytic diffuser' mode where a slight pressure gradient is applied on the gas side in order to force out the liquid entrapped in the pores. Even this approach was not effective.

Nitrophenol was failed to be reduced, this could be probably because of failure of adsorption of either of the reacting components on the surface of the catalyst. As many authors has stated[46], nitrophenol reduction using nanoparticles is based on Langmuir-Hinshelwood mechanism, in which both reacting parties has to be adsorbed on the surface of the catalyst prior to reaction. Under our experimental conditions; if one of the reactants failed to be adsorbed, it is more probabilistic for the reaction not to occur. A strong or weak adsorption of one of the components could also lead to unsuccessful hydrogenation. Meanwhile, under the same experimental conditions (same membrane and concentration), the reduction reaction was found to be proceed very well with $NaBH_4$ reductant. Therefore, it is a reasonable outlook to consider the problem is from unfavorable reaction condition for the reducing agent (hydrogen). In fact water is not a good reaction medium for hydrogenation using hydrogen gas. The solubility of hydrogen in pure methanol and ethanol is significantly higher than in water, hence using either methanol or ethanol solvent for nitrophenol could be the best reaction medium for the hydrogenation of nitrophenol. Therefore, the effect of reaction medium (specially, the effect of solvents such as water, methanol and ethanol) on the hydrogenation of *p*-nitrophenol has to be investigated very well. Because, adsorption of reaction species from their solution on Pd-loaded membrane can affect the adsorption isotherms of catalytic hydrogenation reaction.

5. Conclusion

Incorporating metal nanoparticles into membranes can endow the membranes with additional and specific functions. Surface modification of polyethersulfone membrane by UV-assisted grafting polymerization of acrylic acid has been successfully done. Catalytically active and efficient Pd nanoparticle has been synthesized via intermatrix synthesis. As a model for liquid phase reaction, its catalytic performance was investigated by the reduction of aqueous *p*-nitrophenol to *p*-aminophenol with sodium borohydride as reductant. The catalytic activity of Pd embedded membrane was shown to be directly proportional to the palladium content in the nanocomposite. The catalytic activity of flow through reactor for reduction of nitrophenol outperformed the batch mode of operation, as it was demonstrated by conversion comparison at the same initial concentration nitrophenol and weight of catalyst. This was attributed to the convective flow of reactants directly to the catalyst sites which can provide an intensive contact. An important asset in application of membrane embedded catalysts is the possibility of varying the flux to control the conversion. At lower and moderate range of fluxes, a complete conversion was achieved in FTCMR, but an increase in the flux decreased the conversion, because of insufficient contact time. The effect of initial nitrophenol concentration at the same flux and catalyst has been investigated. In all concentration ranges taken, a lower initial concentration had higher conversion and rate constant, as higher concentration poses surface coverage of the catalyst. Further investigation of p-nitrophenol reduction reactions related to porosity of the grafted layer has to be done.

Photochemical modified commercial hollow fiber microfiltration PES membrane, containing palladium catalyst was also tested for hydrogenation of *p*-NP as a model for Gas/liquid contacting. However, the reaction was not successful, and this could be related to our experimental conditions. Due to the fact that water is not a good reaction medium for hydrogenation reaction using hydrogen gas, the reacting species may be not well adsorbed over the surface of the catalyst. As the solubility of hydrogen in pure methanol and ethanol is significantly higher than in water, testing at either of the solvents could be a solution. This clearly showed that a further investigation has to be done related to the effect of reaction medium (specially, the effect of solvents such as water, methanol and ethanol) on the hydrogenation of *p*-nitrophenol. Because, adsorption of reaction species from their solution on Pd-loaded membrane can affect the adsorption isotherms of catalytic hydrogenation reaction

6. Bibliography

1. M.N. Abu Semana, M.K., Z.I. Bin Ali, N. Hilal, *Reduction of nanofiltration membrane fouling by UV-initiated graft polymerization technique.* Journal of Membrane Science, 2010(355): p. 133–141.
2. Anne Julbe, D.F., Christian Guizard, *Porous ceramic membranes for catalytic reactors-overview and new ideas.* Journal of Membrane Science 2001. **181**: p. 3–20.
3. Sibel Sain Ozdemir, M.G.B., E. Drioli b, *Catalytic polymeric membranes: Preparation and application.* Applied Catalysis, 2006. **307**: p. 167-183.
4. Vladimir V. Pushkarev , Z.Z., Kwangjin An , Antoine Hervier , Gabor A. Somorjai, *Monodisperse Metal Nanoparticle Catalysts: Synthesis, Characterizations, and Molecular Studies Under Reaction Conditions.* Topics in Catalysis, 2012. **55**: p. 1257–1275.
5. Kyungsu Na, Q.Z., Gabor A. Somorjai, *Colloidal Metal Nanocatalysts: Synthesis, Characterization, and Catalytic Applications.* Journal of Cluster Science, 2014. **25**(1): p. 83-114
6. Patricia Ruiz, M.ı.M.n., Jorge Macan´as, Constantin Turta, Denis Prodiusb and Dmitri N. Muraviev, *Intermatrix synthesis of polymer stabilized inorganic nanocatalyst with maximum accessibility for reactants.* The Royal Society of Chemistry, 2010: p. 1751–1757.
7. Julio Bastos-Arrietaa, A.S., Amanda Alonsoa, Maria Mu˜noza, Jorge Macanásb, Dmitri N. Muraviev, *Donnan exclusion driven intermatrix synthesis of reusable polymer stabilized palladium nanocatalysts.* Catalysis Today, 2012. (193): p. 207– 212.
8. Nidal Hilal, L.A.-K., Brian P. Atkin, Victor Kochkodanb, Nelya Potapchenkob, *Photochemical modification of membrane surfaces for (bio)fouling reduction: a nano-scale study using AFM.* Desalination, 2003(158): p. 65-72.
9. James E. Kilduft, S.M., John P. Pieracci , Georges Belfort *Photochemical modification of poly(ether sulfone) and sulfonated poly(sulfone) nanofiltration membranes for control of fouling by natural organic matter* Desalination 2000(132): p. 133-142.
10. Clélia Emin, J.-C.R., Jean-François Lahitte, *Influence of UV grafting conditions and gel formation on the loading and stabilization of palladium nanoparticles in photografted polyethersulfone membrane for catalytic reactions* Journal of Membrane Science, 2014(455): p. 55–63.
11. Silke Ziegler, J.T., Detlev Fritsch, *Palladium modified porous polymeric membranes and their performance in selective hydrogenation of propyne.* Journal of Membrane Science 2001. **187** (71-84).
12. Roduner, E., *Size matters: why nanomaterials are different* Chemical Society Reviews 2006. **35**(7): p. 583-592.
13. Fendler, J., *Colloid Chemical Approach to Nanotechnology.* Korean Journal of Chemical Engineering, 2001. **18**(1): p. 1-13.
14. Neouze, M.-A., *Nanoparticle assemblies: main synthesis pathways and brief overview on some important applications.* Journal of Material Science, 2013. **48**(21): p. 7321-7349.
15. Dingsheng Wang, T.X., Yadong Li *Nanocrystals: Solution-Based Synthesis and Applications as Nanocatalysts.* Nano Research, 2009. **2**(1): p. 30-46.
16. Poovathinthodiyil Raveendran, J.F., and Scott L. Wallen, *Completely "Green" Synthesis and Stabilization of Metal Nanoparticles.* Journal of American Chemical Society, 2003. **125**: p. 13940-13941.
17. Sinfelt, J.H., *Bimetallic catalysts: Discoveries, concepts, and applications* Journal Of The American Chemical Society, 1984. **106**(8).
18. Sudipta Sarkar E. Guibal , F.Q.A.K.S., *Polymer-supported metals and metal oxide nanoparticles:synthesis, characterization, and applications*

Journal of Nanoparticle Research 2012. **14**: p. 1051-1075.

19. Juan M. Campelo Prof., D.L.P., Rafael Luque Dr., José M. Marinas Prof. and Antonio A. Romero Dr., *Sustainable Preparation of Supported Metal Nanoparticles and Their Applications in Catalysis.* Chemistry and Sustainability, 2009. **2**(1): p. 18-45.

20. Bo Denga, J.L., Zhengchi Houa, Side Yaoa, Liuqing Shia, Guoming Lianga, Kanglong Shenga, *Microfiltration membranes prepared from polyethersulfone powder grafted with acrylic acid by simultaneous irradiation*

and *their pH dependence.* Journal of Radiation Physics and Chemistry, 2008. **77**: p. 898-906.

21. Berta Domènech1, M.M., Dmitri N Muraviev1 and Jorge Macanás, *Polymer-stabilized palladium nanoparticles for catalytic membranes: ad hoc polymer fabrication.* Nanoscale Research Letters 2011. **6**(406).

22. Rahimpour, A., *UV photo-grafting of hydrophilic monomers onto the surface of nano-porous PES membranes for improving surface properties*

Desalination 2011. **265** p. 93–101.

23. Roy Bernstein, E.A.n., and Mathias Ulbricht, *UV-Photo Graft Functionalization of Polyethersulfone Membrane with Strong Polyelectrolyte Hydrogel and Its Application for*

Nanofiltration. Journal of American Chemical Society, 2012. **4**: p. 3438–3446.

24. J. Macanása, L.O., M.L. Bruening, M. Mu˜nozd, J.-C. Remigya, J.-F. Lahittea, *Development of polymeric hollow fiber membranes containing catalytic metal nanoparticles.* Catalysis Today, 2010.

25. Westermann, T., *Flow-Through Membrane Microreactor for Intensified Heterogeneous Catalysis.* 2009.

26. Thomas Westermann, T.M., *Flow-through catalytic membrane reactors—Principles and applications*

Chemical Engineering and Processing 2009. **48**: p. 17–28.

27. Nazely Diban, A.T.A., Javier Bilbao, Ane Urtiaga, and Inmaculada Ortiz, *Membrane Reactors for in Situ Water Removal: A Review of Applications*

Industrial and Engineering chemistry research.

28. Roland Dittmeyer, V.H., Kristian Daubb, *Membrane reactors for hydrogenation and dehydrogenation processes based on supported palladium.* Journal of Molecular Catalysis, 2001. **173**: p. 135-184.

29. Kamalesh K. Sirkar, P.V.S., and A. Sarma Kovvali, *Membrane in a Reactor: A Functional Perspective.* Industrial & Engineering Chemistry Research, 1999. **38**: p. 3715-3737.

30. Frank Lipnizki, R.W.F., Po-Kiong Ten, *Pervaporation-based hybrid process: a review of process design, applications and economics*

Journal of Membrane Science, 1999. **153**: p. 183-210.

31. Yuwen Zhang, K.S., Fanlin Zeng, Weizhong Ding, Xionggang Lu, *A novel tubular oxygen-permeable membrane reactor for partial oxidation of CH4 in coke oven gas to syngas*

International Journal of hydrogen energy 2013. **38**: p. 8783-8789.

32. M. A. Al-Juaied, D.L., A. Varma, *Ethylene epoxidation in a catalytic packed-bed membrane reactor: experiments and model.* Chemical Engineering Science, 2001. **56**: p. 395-402.

33. M. Pera-Titusa, M.F., N. Guilhaumea, K. Fiatyb, *Modelling nitrate reduction in a flow-through catalytic membrane contactor:Role of pore confining effects on water viscosity*

Journal of Membrane Science, 2012. **402**: p. 204-216.

34. Nagy, E., *Mass Transfer through a Convection Flow Catalytic Membrane Layer with Dispersed Nanometer-Sized Catalyst*

Industrial & Engineering Chemistry Research, 2010. **49**: p. 1057-1062.

35. M.M. Yousef Motamedhashemia, F.E., Theodore Tsotsis, *Application of a flow-through catalytic membrane reactor (FTCMR) for the destruction of a chemical warfare simulant.* Journal of Membrane Science, 2011(376): p. 119–131.

36. Specchia, G.S.a.V., *Catalytic Ceramic Filters for Flue Gas Cleaning. 2.Catalytic Performance and Modeling Thereof.* Industrial & Engineering Chemistry Research, 1995(34): p. 1480-1487.

37. A. J. Maira, W.N.L., C. Y. Lee, P. L. Yue, C. K. Chan, K. L. Yeung, *Performance of a membrane-catalyst for photocatalytic oxidation of volatile organic compounds.* Chemical Engineering Science 2003. **58** p. 959 – 962.

38. Masayoshi Kobayashi, J.T., Tohru Kanno, Jun-ichi Horiuchi and Kiyosi Tada, *Dramatic innovation of propene epoxidation efficiency derived from a forced flow membrane reactor.* J Chem Technology and Biotechnology 2003. **78**: p. 303–307.

39. C. Lange, S.S., B. Tesche, andW. F. Maier, *Selective Hydrogenation Reactions with a Microporous Membrane Catalyst, Prepared by Sol–Gel Dip Coating.* Journal of Catalysis 1998. **175**: p. 280–293

40. A.M. Ramachandra, Y.L., Y.H. Ma, W.R. Moser, A.G. Dixon,
Oxidative coupling of methane in porous Vycor membrane reactors. Journal of Membrane Science 1996. **116** p. 253-264.

41. Oleg M. Ilinitch a, F.P.C., Ludmila V. Nosova , Evgeni N. Gribov, *Catalytic membrane in reduction of aqueous nitrates: operational principles and catalytic performance.* Catalysis Today, 2000. **56**: p. 137–145.

42. T.N. Shah, S.M.C.R., *Esterification catalysis using functionalized membranes.* Journal of Applied Catalysis 2005. **296**: p. 12–20.

43. Jian Xu, D.B., *Modeling of Fe/Pd Nanoparticle-Based Functionalized Membrane Reactor for PCB Dechlorination at Room Temperature*
Journal of Physical chemistry 2008. **112**: p. 9133–9144.

44. Lu Ouyanga, D.M.D., Seth R. Hogga, Jorge Macanásb, Jean-Francois Lahitteb, Merlin L. Brueninga, *Catalytic hollow fiber membranes prepared using layer-by-layer adsorption of polyelectrolytes and metal nanoparticles.* Catalysis Today, 2010.

45. Hanyang Li, H.J., Rizhi Chen, Yong Wang, and Weihong Xing, *Enhanced Catalytic Properties of Palladium Nanoparticles Deposited on a Silanized Ceramic Membrane Support with a Flow-Through Method*
Industrial & Engineering Chemistry Research, 2013. **52**: p. 14099–14106.

46. Stefanie Wunder, F.P., Yan Lu, Yu Mei, and Matthias Ballauff, *Kinetic Analysis of Catalytic Reduction of 4-Nitrophenol by Metallic Nanoparticles Immobilized in Spherical Polyelectrolyte Brushes*
Journal of Physical Chemistry, 2010. **114**: p. 8814–8820.

47. Fengling Xia, X.X., Xichuan Li, Lei Zhang, Li Zhang, Wei Wang, Yu Liu, and Jianping Gao, *Preparation of bismuth nanoparticles in aqueous solution and its catalytic performance for the reduction of 4–nitrophenol.* Industrial & Engineering Chemistry Research, 2014.

48. Mulisa Nemanashi, R.M., *Synthesis and characterization of Cu, Ag and Au dendrimer-encapsulated nanoparticles and their application in the reduction of 4-nitrophenol to 4-aminophenol* Journal of Colloid and Interface Science, 2013. **389**: p. 260–267.

49. Xuzhe Wang , J.F., Minghuan Wang ,Yajie Wang , Zhimin Chen , Jianan Zhang, Jiafu Chen • Qun Xu, *Facile synthesis of Au nanoparticles supported on polyphosphazene functionalized carbon nanotubes for catalytic*
reduction of 4-nitrophenol. Journal of Materials Science, 2014. **49**(14): p. 5056-5065

50. Roland Dittmeyer, K.S., and Martin Reif, *A review of catalytic membrane layers for gas/liquid reactions*
Topics in Catalysis, 2004. **29**: p. 1-25.

51. David M. Dotzauer, J.D., Lei Sun, and Merlin L. Bruening, *Catalytic Membranes Prepared Using Layer-by-Layer Adsorption of Polyelectrolyte/Metal Nanoparticle Films in Porous Supports.* Nano Letters, 2006. **6** p. 2268–2272.

52. Christopher A. Crock, A.R.R., Wenqian Shan , Volodymyr V. Tarabara, *Polymer nanocomposites with graphene-based hierarchical fillers as materials for multifunctional water treatment membranes*
water research 2013. **47**: p. 3 9 8 4 -3 9 9 6.
53. V.Y. Dindore, D.W.F.B., F.H. Geuzebroek, G.F. Versteeg, *Membrane–solvent selection for CO2 removal using membrane gas–liquid contactors*
Separation and Purification Technology 2004. **40**: p. 133-145.
54. A. Bottino, G.C., A. Comitea, R. Di Feliceb, *Polymeric and ceramic membranes in three-phase catalytic membrane reactors for the hydrogenation of methylenecyclohexane.* Desalination 2002. **144**: p. 41 I-416.
55. Detlev Fritsch , G.B., *Development of catalytically reactive porous membranes for the selective hydrogenation of sunflower oil.* Catalysis Today 2006. **118**: p. 121–127.
56. Rizhi Chen, Y.J., Weihong Xing, and Wanqin Jin, *Fabrication and Catalytic Properties of Palladium Nanoparticles Deposited on a Silanized Asymmetric Ceramic Support.* Industrial & Engineering Chemistry Research, 2011. **50**: p. 4405–4411.
57. C. V. Rode, M.J.V., and R. V. Chaudhari, *Synthesis of p-Aminophenol by Catalytic Hydrogenation of Nitrobenzene.* Organic Process Research & Development 1999. **3**: p. 465-470.
58. Rizhi Chen, Y.D., Weihong Xing, and Wanqin Jin, *Effect of initial solution apparent pH on the performance of submerged hybrid system for the p-nitrophenol hydrogenation.* Korean Journal of Chemical Engineering, 2009. **26**(6): p. 1580-1584.
59. Rahat Javaid, S.-i.K., Akira Suzuki and Toshishige M. Suzuki, *Simple and rapid hydrogenation of p-nitrophenol with aqueous formic acid in catalytic flow reactors*
Beilstein Journal of Organic chemistry, 2013. **9**: p. 1156–1163.
60. Rizhi Chen, Y.J., Weihong Xing, and Wanqin Jin, *Preparation of Palladium Nanoparticles Deposited on a Silanized Hollow Fiber Ceramic Membrane Support and Their Catalytic*
Properties. Industrial & Engineering Chemistry Research, 2013. **52**: p. 5002–5008.
61. M.N. Abu Seman, M.K., N. Hilal, *Comparison of two different UV-grafted nanofiltration membranes prepared for reduction of humic acid fouling using acrylic acid and N-vinylpyrrolidone.* Desalination 2012. **287**: p. 19–29.

Appendix

Combined Diffusion and Convection mass transport with reaction

The differential mass transport across a reactive membrane layer with constant transport parameters through combined mass transport with chemical reaction is described by a continuity equation for Cartesian coordinate system. For reactant species A

$$C \left(\frac{\partial X_A}{\partial t} + V_x \frac{\partial X_A}{\partial x} + V_y \frac{\partial X_A}{\partial y} + V_z \frac{\partial X_A}{\partial z} \right) = C * D \left(\frac{\partial^2 X_A}{\partial x^2} + \frac{\partial^2 X_A}{\partial y^2} + \frac{\partial^2 X_A}{\partial z^2} \right) + r_A \qquad (A)$$

Where C is the concentration, x is molar fraction, D is the diffusion coefficient in the membrane (m^2/s), r is rate of reaction, and V is the convective velocity (m/s) through the

membrane. For steady state system with a convective flow in X direction(only the velocity in x direction), the above equation becomes

$$V_x \frac{dC_A}{dx} = D \frac{d^2 C_A}{dx^2} + r_A \;,$$

$$D \frac{d^2 C_A}{dx^2} - V_x \frac{dC_A}{dx} - r_A = 0, \quad \text{for Pseudo first order reaction } r = -K_{app}{}^* C_A$$

$$D \frac{d^2 C_A}{dx^2} - V_x \frac{dC_A}{dx} - Kapp * CA = 0$$

Introducing dimensionless length $\varepsilon = x/\delta$, where δ is catalytic membrane layer.

$$\frac{d^2 C_A}{d\varepsilon^2} - \frac{V*\delta}{D} * \frac{dC_A}{d\varepsilon} - \frac{K_{app}\delta^2}{D} C_A = 0$$

Introducing peclet number and a reaction modulus which is a dimensionless group representing the relative influence of the chemical reaction and diffusion. Reaction modulus is given by $\varnothing^2 = \frac{K_{app}\delta^2}{D}$

$$P_e = \frac{V * \delta}{D}$$

Substituting these two terms in to the above governing equation,

$$\frac{d^2 C_A}{d\varepsilon^2} - P_e \frac{dC_A}{d\varepsilon} - \varnothing^2 C_A = 0$$

Where, C_A is the concentration of reactant 'A' and , δ is the thickness of the catalytic membrane layer, $P_{e,}$ is peclet number, $\varepsilon = x/\delta$ is dimensionless thickness of the membrane.

Using standard ordinary differential equation solution methods, the above second order differential equations cab be solved.

Let $C_A = m * exp\left[\frac{P_e \varepsilon}{2}\right]$

$$\frac{dC_A}{d\varepsilon} = exp\left[\frac{P_e \varepsilon}{2}\right]\frac{dm}{d\varepsilon} + \frac{mP_e}{2} exp\left[\frac{P_e \varepsilon}{2}\right]$$

$$\frac{d^2 C_A}{d\varepsilon^2} = \frac{d}{d\varepsilon}\left(exp\left[\frac{P_e \varepsilon}{2}\right]\frac{dm}{d\varepsilon} + \frac{mP_e}{2} exp\left[\frac{P_e \varepsilon}{2}\right]\right)$$

$$\frac{d^2C_A}{d\varepsilon^2} = exp\left[\frac{P_e\varepsilon}{2}\right]\frac{d^2m}{d\varepsilon^2} + \frac{P_e}{2}exp\left[\frac{P_e\varepsilon}{2}\right]\frac{dm}{d\varepsilon} + \frac{P_e}{2}exp\left[\frac{P_e\varepsilon}{2}\right]\frac{dm}{d\varepsilon} + \frac{mP^2_e}{4}exp\left[\frac{P_e\varepsilon}{2}\right]$$

Substituting in to the above equation gives, the following simplified differential equation.

$$\frac{d^2m}{d\varepsilon^2} - \varphi^2m = 0 \text{ , where } \varphi^2 = \frac{P^2_e}{4} + \emptyset^2$$

The solution of the above second order differential equation is a hyperbolic function with the following form

$$m = Acosh(\varepsilon\varphi) + Bsinh(\varepsilon\varphi), \text{ or,}$$

$$C_A = A * exp\left[\frac{P_e\varepsilon}{2}\right]cosh(\varepsilon\varphi) + B * exp\left[\frac{P_e\varepsilon}{2}\right]sinh(\varepsilon\varphi)$$

The constant parameters A and B are determined by the boundary conditions, without external diffusive mass transfer resistances,

The boundary conditions are,

$\varepsilon= 0$, $C_A= C_{A0,}$ $\quad x = \delta \text{ or } \varepsilon=1, \frac{dC_A}{d\varepsilon} = 0$, because at the end of the catalytic layer, the concentration does not change any more.

Solving at the boundary equations, the concentration profile across the layer is given by as a function of P_e and dimensionless length.

$$\frac{C_A}{C_{A0}} = exp\left[\frac{P_e\,\varepsilon}{2}\right]\left[\frac{Sinh(\varphi(1-\varepsilon)) * \frac{P_e}{2} + \varphi cosh[\varphi(1-\varepsilon)]}{\frac{P_e}{2}Sinh\varphi + \varphi cosh\varphi}\right]$$

Where, $\varphi = \sqrt{\left(\frac{P_e^2}{4} + \emptyset^2\right)}$, $\emptyset^2 = \frac{K_{app}\delta^2}{D}$, and $P_e = \frac{V*\delta}{D}$

This equation shows how the concentration is changing across the catalytic layer. Meanwhile, we can predict the concentration distribution at the end of the membrane ($\varepsilon= 1$), as function of initial concentration, peclet number and reaction modules $\emptyset$ with the following equation.

$$\frac{C_A}{C_{A0}} = \frac{\varphi * exp\left[\frac{P_e}{2}\right]}{\frac{P_e}{2}Sinh\varphi + \varphi cosh\varphi}$$

Convection mass transport with reaction

If we only neglect the diffusion term, for steady state equation A becomes

$$V_x \frac{dC_A}{dx} = r_A$$

$$V_x \frac{dC_A}{dx} = -K_{app}C_A, \text{ for the membrane thickness } \delta, \text{ and convective velocity (m/h) is given by}$$

$V_x = J_v$, where J_v is the flux in $(m^3 \, h^{-1} m^{-2})$

$$C_A = C_0 \exp\left[\frac{K_{app}\delta}{J_v}\right]$$